iScience

CellPress
OPEN ACCESS

Article

AKAP8 promotes ovarian cancer progression and antagonizes PARP inhibitor sensitivity through regulating hnRNPUL1 transcription

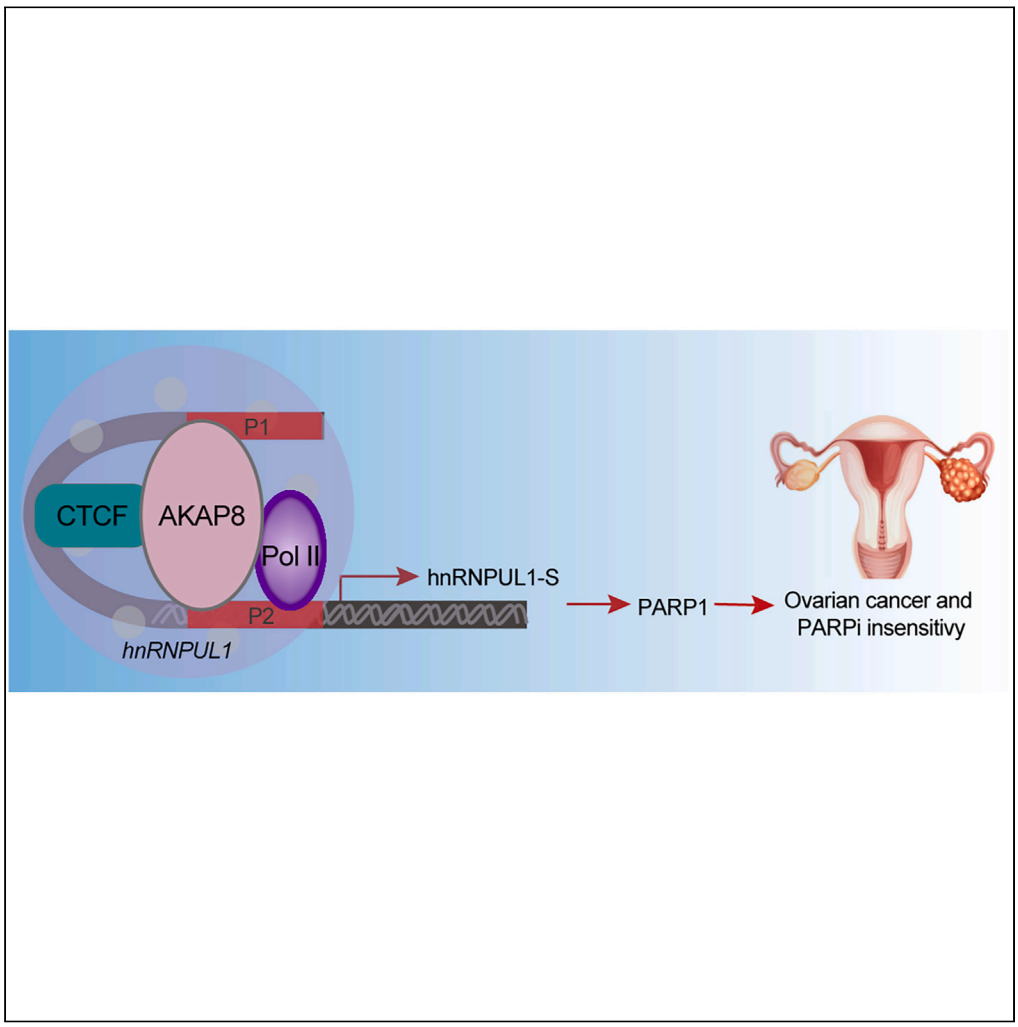

Youchaou Mobet, Haocheng Wang, Qinglv Wei, ..., Jing Xu, Tao Liu, Ping Yi

anti1988@163.com (T.L.)
yiping@cqmu.edu.cn (P.Y.)

Highlights

AKAP8 plays an oncogenic role in ovarian cancer

AKAP8 condensation promotes ovarian cancer, which is crucial for mediating hnRNPUL1 transcription

AKAP8 decreases PARPi sensitivity through hnRNPUL1 in ovarian cancer

Mobet et al., iScience 27, 109744
May 17, 2024
https://doi.org/10.1016/j.isci.2024.109744

iScience

CellPress
OPEN ACCESS

Article

AKAP8 promotes ovarian cancer progression and antagonizes PARP inhibitor sensitivity through regulating hnRNPUL1 transcription

Youchaou Mobet,[1,2,5] Haocheng Wang,[1,5] Qinglv Wei,[1,3] Xiaoyi Liu,[1] Dan Yang,[1] Hongyan Zhao,[1] Yu Yang,[1] Rosalie Anne Ngono Ngane,[2] Jacob Souopgui,[4] Jing Xu,[1] Tao Liu,[1,*] and Ping Yi[1,6,*]

SUMMARY

Ovarian cancer (OC) is the highest worldwide cancer mortality cause among gynecologic tumors, but its underlying molecular mechanism remains largely unknown. Here, we report that the RNA binding protein A-kinase anchoring protein 8 (AKAP8) is highly expressed in ovarian cancer and predicts poor prognosis for ovarian cancer patients. AKAP8 promotes ovarian cancer progression through regulating cell proliferation and metastasis. Mechanically, AKAP8 is enriched at chromatin and regulates the transcription of the specific hnRNPUL1 isoform. Moreover, AKAP8 phase separation modulates the hnRNPUL1 short isoform transcription. Ectopic expression of the hnRNPUL1 short isoform could partially rescue the growth inhibition effect of AKAP8-knockdown in ovarian cancer cells. In addition, AKAP8 modulates PARP1 expression through hnRNPUL1, and AKAP8 inhibition enhances PAPR inhibitor cytotoxicity in ovarian cancer. Together, our study uncovers the crucial function of AKAP8 condensation-mediated transcription regulation, and targeting AKAP8 could be potential for improvement of ovarian cancer therapy.

INTRODUCTION

Ovarian cancer has the highest worldwide cancer mortality within gynecologic tumors, which has poor outcomes, increasing incidence and mortality with almost 140,000 deaths per year.[1,2] The high relapse and mortality rates of ovarian cancer are attributable to late diagnosis and the development of drug resistance in most patients.[3] One of the factors for ovarian tumors' propensity to recur is genomic instability, and about 50% of high-grade serous ovarian cancers (HGSOC) have a homologous recombination deficit.[4] The risk of ovarian cancer is associated with DNA damage.[5,6] Poly ADP-ribose polymerase (PARP) inhibitors (PARPis) are selective PARP nuclear proteins that recognize DNA damage and encourage repair.[7] In the last two decades, PARPis have been applied as promising drug candidates for the front-line treatment for maintenance therapy and in patients with relapse, but limited therapeutic efficacy was observed.[7,8] Despite the curative benefits of PARPis, there is still a therapeutic challenge because long-term survival rates for patients with ovarian cancer remain unsatisfactory.

AKAP8 also called AKAP95, is the main nuclear member of the diverse A-kinase anchoring proteins (AKAPs) family, which could bind to protein kinase A (PKA) and control cellular signaling.[9,10] The complex PKA-AKAP8 participates in remodeling chromatin during mitosis.[11] It has been demonstrated that AKAP8 is associated with chromatin and nuclear matrix which has a remarkable activity in promoting chromatin transcription supporting the biological significance of AKAP8 regulating gene expression.[12,13] Jiang and collaborators showed that AKAP8 is a chromatin-associated protein regulating histone 3 lysine 4 tri-methylation (H3K4me3) enrichment which is associated with gene activation.[14] As a highly abundant nuclear protein, AKAP8 could act as a regulator of transcription and can modify the activity of splicing factors, including its pre-mRNA splicing.[13,15]

AKAP8 interacts with heterogeneous nuclear ribonucleoprotein (hnRNP) protein groups and directly regulates pre-mRNA splicing.[13] Hu et al. reported that AKAP8 acts as an RNA-binding protein and interacts with hnRNPM to cooperatively regulate alternative splicing in breast cancer.[15] Dysregulation of AKAP8 has been implicated in cancers including breast cancer,[15,16] colorectal cancer,[17,18] and lung cancer.[19] In lung cancer, AKAP8 binds to cyclin E1/E2 and inhibits their degradation, thus promoting their protein expression and G1/S conversion.[19] AKAP8 expression is correlated with Epac1, which is increased in breast cancer. In contrast, it has been reported that AKAP8 promotes CD44 exon skipping, acting as a tumor suppressor gene in triple-negative breast cancer.[15] However, the critical role of AKAP8 in ovarian cancer and whether AKAP8-mediated gene transcription is involved in its tumor-regulating function have not been investigated.

[1]Department of Obstetrics and Gynecology, The Third Affiliated Hospital of Chongqing Medical University, Chongqing 401120, China
[2]Laboratory of Biochemistry, Faculty of Science, University of Douala, P.O. Box 24157, Douala, Cameroon
[3]Chongqing Key Laboratory of Child Infection and Immunity, Children's Hospital of Chongqing Medical University, Chongqing 400014, China
[4]Department of Molecular Biology, Institute of Biology and Molecular Medicine, IBMM, Université Libre de Bruxelles, Gosselies Campus, 6041 Gosselies, Belgium
[5]These authors contributed equally
[6]Lead contact
*Correspondence: anti1988@163.com (T.L.), yiping@cqmu.edu.cn (P.Y.)
https://doi.org/10.1016/j.isci.2024.109744

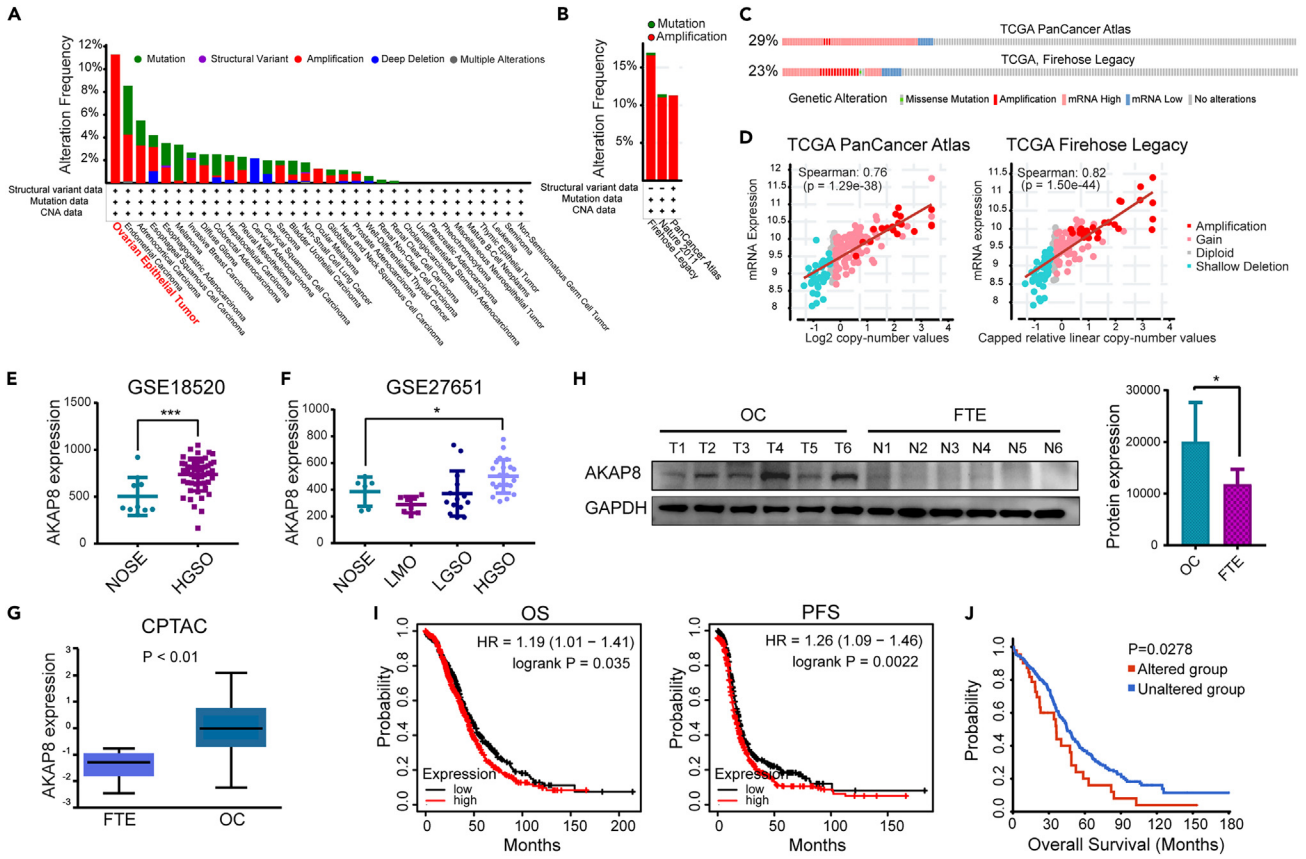

Figure 1. Increased AKAP8 expression is associated with poor prognosis of ovarian cancer patients

(A) Gene mutation rates and alteration frequency analysis of AKAP8 in cancers according to the cBioPortal datasets.

(B) Gene alteration frequency analysis of AKAP8 in ovarian cancer according to three independent TCGA ovarian cancer cohorts.

(C) AKAP8 genetic alteration in two TCGA ovarian cancer cohorts.

(D) Correlation between AKAP8 mRNA expression and gene amplification in TCGA ovarian cancer cohorts.

(E and F) RNA level analysis of AKAP8 in ovarian cancer tissues according to two GEO datasets. NOSE: normal ovarian surface epithelium, HGSO: high-grade serous ovarian cancer, LMO: low metastasis ovarian cancer, LGSO: low-grade serous ovarian cancer.

(G) Protein level analysis of AKAP8 in ovarian cancer tissues and fallopian tube epithelium according to the CPTAC database.

(H) Representative images of AKAP8 protein levels (left) and quantity analysis (right) in fresh ovarian tumor samples and fallopian tube epithelium samples by western blot. OC: ovarian cancer.

(I) Kaplan-Meier analysis for OS and PFS (Affiy ID:203848) of the correlations between AKAP8 expression levels with ovarian cancer patient's prognosis.

(J) Survival analysis of ovarian cancer patients with altered or unaltered AKAP8 gene according to the TCGA database.

In the present study, we outline the role and molecular mechanism of AKAP8 and highlight the abilities of AKAP8 to promote ovarian cancer through regulating the transcription of the specific hnRNPUL1 short isoform (hnRNPUL1-S). hnRNPUL1-S is shown to be considerably over-expressed in ovarian cancer, which promotes the growth and metastasis of ovarian cancer cells. Importantly, we provide evidence that AKAP8 condensates in ovarian cancer cells and the 101–210 region of AKAP8, which contributes to its liquid-liquid phase separation (LLPS), is crucial for its activity in regulating the specific hnRNPUL1 isoform transcription and ovarian tumorigenesis. AKAP8-mediated hnRNPUL1-S transcriptional activation could regulate PARP1 expression and decrease the PARPi niraparib sensitivity in cancer ovarian cells. Thus, our study uncovers the tumor-promoting role of AKAP8 phase separation in ovarian cancer through regulating the specific hnRNPUL1 isoform transcription.

RESULTS

Overexpression of AKAP8 in ovarian cancer is linked to a poor prognosis for patients

To investigate the role of AKAP8 in ovarian cancer, we first assessed AKAP8's genetic modification and expression level using the cBioPortal database (TCGA pan-cancer dataset, https://www.cbioportal.org). AKAP8 was subjected to amplification and mutation in different cancers, among which the highest amplification frequency occurred in ovarian cancer (Figure 1A). In three independent TCGA ovarian cancer cohorts, AKAP8 was amplified with its mRNA upregulation, and gene amplification contributed to upregulation of AKAP8 mRNA (Figures 1B–1D, S1A,

and S1B). Using two GEO cohort databases including (GSE18520, and GSE27651), we also analyzed the mRNA expression of AKAP8 in ovarian cancer and observed that this gene's expression was markedly elevated in this disease (Figures 1E and 1F). Meanwhile, AKAP8 mRNA level was increased in high-grade serous ovarian cancer than in low-grade serous ovarian cancer (Figure 1F).

In addition, the protein level of AKAP8 was compared between ovarian cancer tissues and fallopian tube epithelium (FTE) tissues according to the Clinical Proteomic Tumor Analysis Consortium (CPTAC) database (https://proteomics.cancer.gov/programs/cptac). We found that the expression of AKAP8 protein level was significantly higher in ovarian cancer tissues (Figure 1G). Consistently, western blot assay confirmed that the expression of AKAP8 was significantly higher in the fresh ovarian tumor samples compared with the control tissues (Figure 1H).

To investigate the link between AKAP8 expression and ovarian cancer patients' prognosis, we performed survival analysis through the Kaplan-Meier Plotter ovarian cancer database (https://kmplot.com/analysis/index.php?p=service&cancer=ovar) and observed that patients with higher AKAP8 expression had worse overall survival and disease-free survival (Figure 1I). Similar results were observed according to the TCGA database (Figure S1C). As gene amplification contributed to AKAP8 upregulation, we analyzed the survivals of patients with AKAP8 amplification and found that these AKAP8-altered patients underwent worse prognosis (Figure 1J). These findings show that AKAP8 is over-expressed in ovarian cancer and that it is linked to a bad outcome for patients with ovarian cancer.

AKAP8 promotes the growth and metastasis of ovarian cancer cells *in vitro* and *in vivo*

To study the functions of AKAP8 in ovarian cancer, a series of *in vitro* and *in vivo* experiments were carried out. We initially generated OVCAR3 and SKOV3 cells with stable AKAP8 overexpression, and we performed a western blot analysis to examine the protein level of AKAP8 in ovarian cancer cells (Figure S2A). CCK-8 assays showed that increased AKAP8 expression in OVCAR3 and SKOV3 cells significantly promoted cell proliferation (Figure S2B). Similar patterns were witnessed in colony formation assays (Figures S2C and S2D). Moreover, transwell assays indicated that the migration and invasion ability of OVCAR3 and SKOV3 cells over-expressing AKAP8 was strongly elevated (Figures S2E and S2F).

After that, we attempted to describe the ovarian cancer cell's alteration of cellular phenotypes upon AKAP8 depletion. In both OVCAR3 and SKOV3 cells, AKAP8 was knocked down by two shRNAs (Figure 2A). After AKAP8 knockdown, OVCAR3, and SKOV3 cells' growth was strongly inhibited compared to the control cells according to the colony formation and CCK-8 assays (Figures 2B and 2D). Additionally, cell migration and invasion experiments showed that OVCAR3 and SKOV3 cells' ability to migrate and invade was compromised by AKAP8 loss (Figures 2E and 2F). Based on these results, AKAP8 is crucial for the growth, migration, and invasion of ovarian cancer cells.

Both the subcutaneous tumorigenesis and the peritoneal metastatic xenograft were used to assess the oncogenic role of AKAP8 in ovarian cancer *in vivo*. Firstly, nude mice were subcutaneously injected with control and AKAP8-deficient OVCAR3 cells. The mice were killed after four weeks, and the tumors were isolated. Smaller tumors were derived from the AKAP8-deficient groups than the control group (Figure 2G). In mice with AKAP8 depleted compared to control mice, the average tumor volume and weight were significantly reduced (Figures 2H and 2I). After four weeks following the injection, we examined the peritoneal metastasis of ovarian cells. The mice injected with AKAP8-deficient cells revealed a substantially reduced number of metastatic foci compared with the control mice (Figure 2J). Together, these findings show that AKAP8 plays an oncogenic role in ovarian cancer by regulating cell proliferation and metastasis both *in vitro* and *in vivo*.

AKAP8 regulates the transcription of hnRNPUL1 in an isoform-specific manner

Because AKAP8 was shown to be involved in alternative splicing of pre-mRNA,[15] we performed an RNA-sequencing analysis after AKAP8 knockdown by two shRNA (shA8-1 and shA8-2) in ovarian cancer cell lines. The DEX sequencing method was used for alternative splicing analysis.[30] Results showed that a set of mRNA splicing patterns was changed upon AKAP8 depletion (Figure 3A). We next validated that several AKAP8-regulated the differential exon usages in both OVCAR3 and SKOV3 cells. RT-PCR results showed that different isoforms of hnRNPUL1, CREM, and PSPH were significantly altered in AKAP8-silenced OVCAR3 and SKOV3 cells (Figure 3B). Intriguingly, the differential first exon usage of hnRNPUL1 resulted in different transcripts and AKAP8 knockdown decreased the expression of the short isoform but not the long isoform (Figure 3B). Western blot assays showed that AKAP8 depletion reduced the protein expression of hnRNPUL1, and conversely AKAP8 overexpression could up-regulate hnRNPUL1 expression (Figure 3C).

To further explore whether AKAP8 regulated hnRNPUL1 through interacting its mRNA and regulating its splicing, AKAP8 eCLIP-sequencing was conducted with OVCAR3 cell lines over-expressing AKAP8, and data analysis revealed that AKAP8 mainly bound introns of protein-coding genes (Figures S3A and S3B). Intriguingly, no AKAP8-binding sites were found in hnRNPUL1 pre-mRNA (Figure 3D). AKAP8 RIP-qPCR also showed that no interaction between AKAP8 and hnRNPUL1 mRNA in ovarian cancer cells (Figure S3C), suggesting that AKAP8 regulates expression of the specific hnRNPUL1 isoform but not through the direct splicing regulation.

Previous studies demonstrated that AKAP8 was involved in transcriptional regulation through interacting with the transcription factor complex.[14] Thus, we speculated that AKAP8 might regulate hnRNPUL1 transcription in ovarian cancer cells. To verify this, we used a nucleocytoplasmic separation experiment to identify AKAP8's cellular localization. Results showed that AKAP8 was mainly localized in the nucleus and enriched in chromatin in an RNA-dependent manner (Figure S3D). Then, we performed AKAP8 ChIP assays to confirm whether AKAP8 is bound to the promoter of hnRNPUL1. Visual analysis of the ENCODE online ChIP-seq database (https://www.encodeproject.org/experiments/ENCSR279NEA/) predicted that AKAP8 could bind to eight potential sites at the hnRNPUL1 promoter (Figure 3E). ChIP-PCR results showed that AKAP8 substantially bound to region 3 at the promoter of hnRNPUL1 (Figure 3F).

As AKAP8 specifically regulated the hnRNPUL1 isoform expression, we next attempted to decode how AKAP8 regulated the transcription of the specific hnRNPUL1 isoform. Alternative promoter contributes to the different 5′ end of transcripts, and thus we analyzed the effect of AKAP8 on distinct regions of hnRNPUL1 promoter according to the isoforms. A dual luciferase reporter assay was performed by constructing

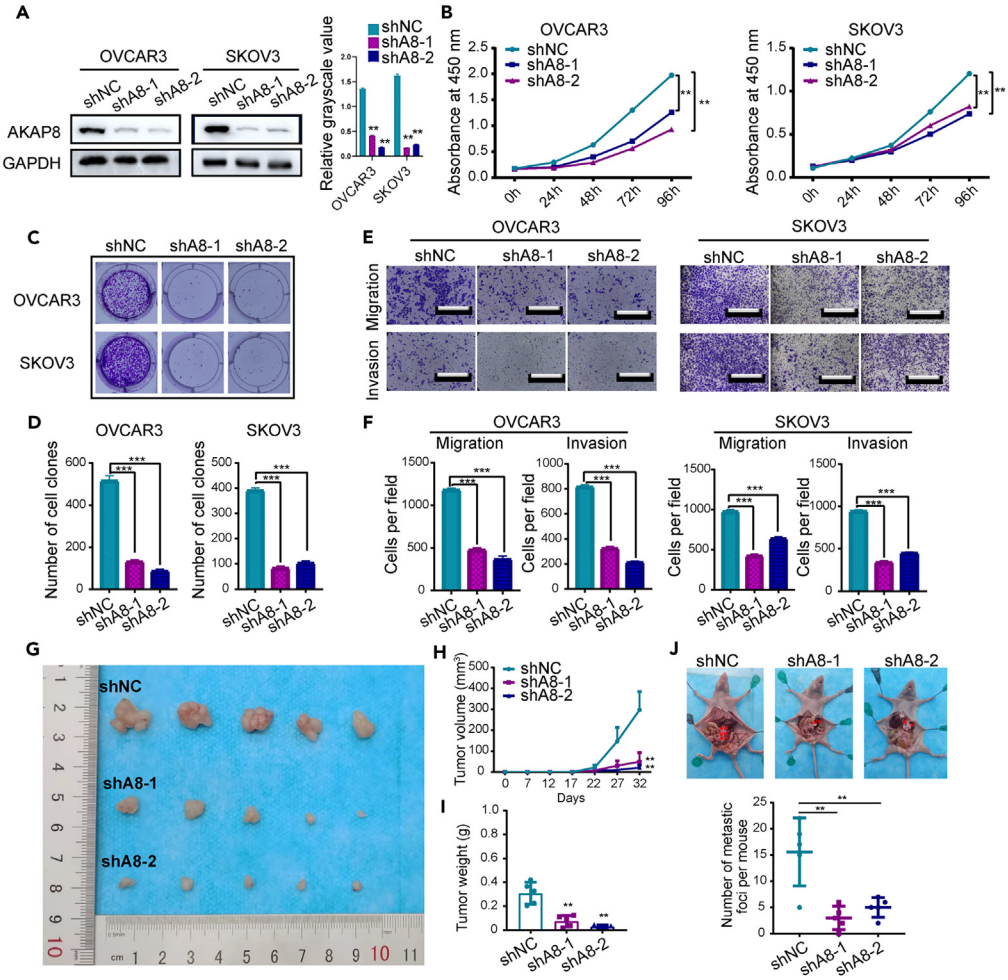

Figure 2. Knockdown of AKAP8 decreases cell proliferation and metastasis of ovarian cancer cells *in vitro* and *in vivo*

(A) Representative western blot of protein levels after AKAP8 knockdown by two independent shRNAs in ovarian cancer cells (left) and relative grayscale protein value (right).

(B) CCK-8 assays detecting the inhibition of ovarian cancer cells' growth upon AKAP8 knockdown.

(C) Representative colony formation images in ovarian cancer cells as described in (A).

(D) The quantification of colonies numbers from (C).

(E and F) Representative images and quantification of migration and invasion of ovarian cancer cells by transwell assays. Scale bar, 200 μm.

(G) Representative images of tumorigenesis xenograft model using mice injected with AKAP8-depleted or control OVCAR3 cells.

(H and I) Tumor volume and tumor weight for xenograft excised from (G).

(J) Representative images of the peritoneal metastatic xenograft model (upper) and the number of ovarian metastasis (bottom) derived from AKAP8 knockdown or control OVCAR3 cells. Data were shown as mean ± SD from three independent experiments. $^{**}p < 0.01$, $^{***}p < 0.001$.

the reported plasmids with the different regions of hnRNPUL1 promoter pGL3-hnRNPUL1-S, pGL3-hnRNPUL1-S-Delete, pGL3-hnRNPUL1-L (Figure 3G). The luciferase activity was detected in control or AKAP8-depleted ovarian cancer cells transfected with these plasmids, respectively. Depletion of AKAP8 significantly decreased the luciferase activity in ovarian cancer cells transfected with pGL3-hnRNPUL1-S, but not pGL3-hnRNPUL1-S-Delete or pGL3-hnRNPUL1-L (Figure 3H). Conversely, overexpression of AKAP8 could enhance the activity of cells transfected with pGL3-hnRNPUL1-S, but not pGL3-hnRNPUL1-S-Delete or pGL3-hnRNPUL1-L, suggesting AKAP8 specifically regulated the expression of a gene with hnRNPUL1-S promoter (Figure 3I).

To further confirm AKAP8-mediated transcriptional regulation of hnRNPUL1, we performed Pol II ChIP-qPCR in OVCAR3 cells upon AKAP8 knockdown and found that AKAP8 knockdown decreased the enrichment of Pol II at hnRNPUL1 promoter (Figure 3J). AKAP8 was demonstrated to be a chromatin-associated protein,[12] which plays an important role in gene expression through regulating histone modifications.[14] Thus, we performed H3K4me3 and CCCTC-binding factor (CTCF) ChIP assays followed by RT-qPCR detection in ovarian cancer cells upon AKAP8 knockdown. After AKAP8 knockdown, the enrichment of H3K4me3 and CTCF at the hnRNPUL1-S promoter was down-regulated (Figures S3E and S3F). Together, these findings imply that AKAP8 regulates the transcription of the specific hnRNPUL1 isoform.

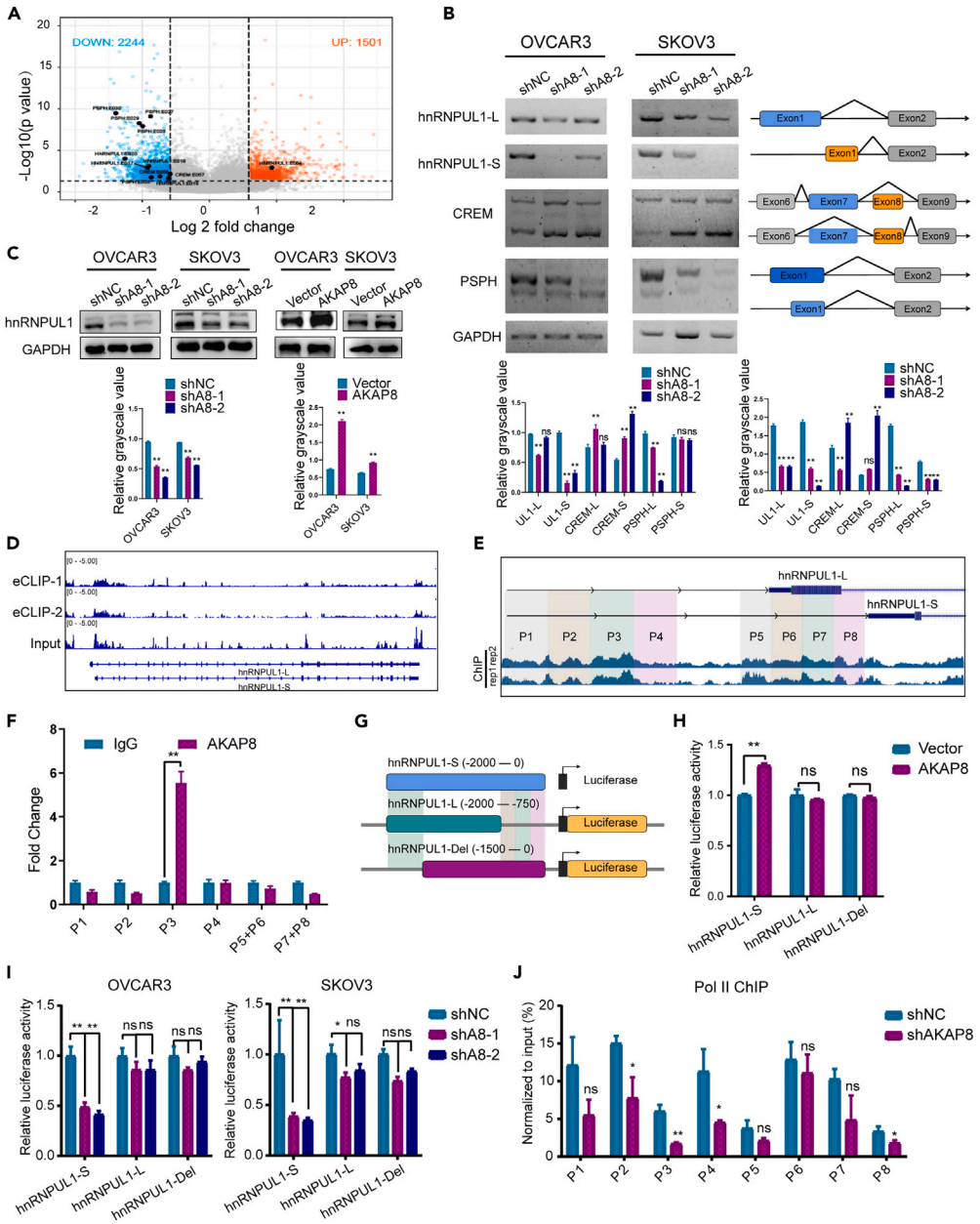

Figure 3. AKAP8 regulates the transcription of the specific hnRNPUL1 isoform

(A) Volcano plot of genes with differential exon usages upon AKAP8 knockdown (FC > 1.5 & $p < 0.05$).

(B) Representative RT-PCR different variant' expression in ovarian cancer cells upon AKAP8 knockdown (left), their schematic transcription variants (right) and relative grayscale mRNA value (below). Constitutive exons are shown as blue, gray, and orange boxes coding regions. GAPDH was used as control.

(C) Representative western blot of hnRNPUL1 protein levels in ovarian cancer cells upon AKAP8 knockdown or overexpression (upper) and relative grayscale protein value (below).

(D) eCLIP-sequencing analysis detecting the enrichment of AKAP8 with hnRNPUL1 RNA in ovarian cancer cells.

(E) Schematic diagram of the different promoter regions of hnRNPUL1-L and hnRNPUL1-S.

(F) The interaction between AKAP8 and hnRNPUL1 promoter was confirmed by ChIP assays.

(G) Schematic representation of different regions of hnRNPUL1 promoter which are inserted into the reporter vector.

(H) Relative luciferase activity of AKAP8 overexpression in ovarian cancer cells co-transfected with plasmids described in (G).

(I) Relative luciferase activity of ovarian cancer cells transfected with the plasmid containing the different promoter regions of hnRNPUL1 upon AKAP8 depletion.

(J) ChIP assays revealed the enrichment of Pol II at the promoter of hnRNPUL1 upon AKAP8 depletion. Data were shown as mean ± SD. *$p < 0.05$, **$p < 0.01$, ns, not significant.

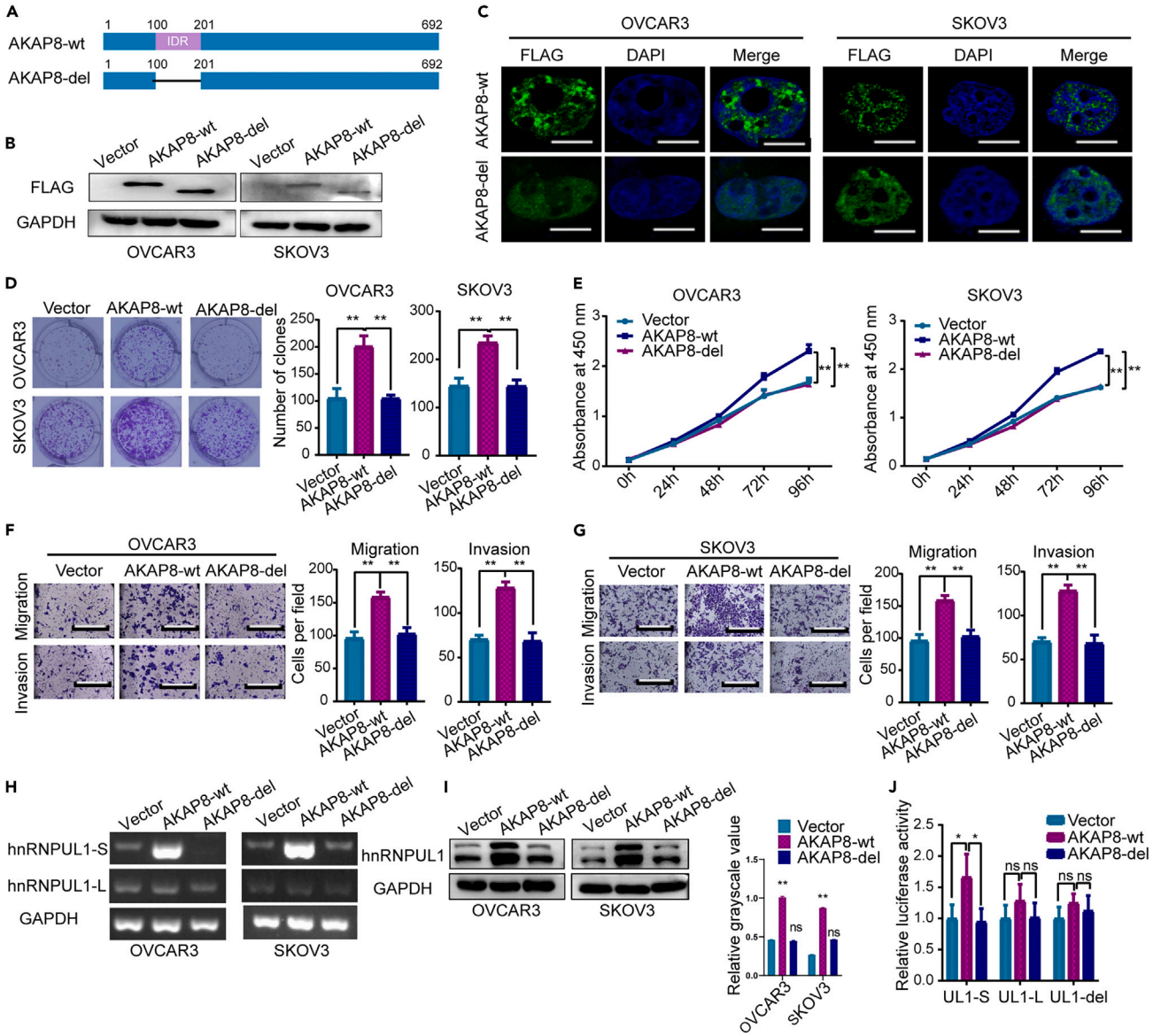

Figure 4. AKAP8 condensation is crucial for its activity of regulating hnRNPUL1 expression in ovarian cancer

(A) Schematic of AKAP8-wt and AKAP8-delete.

(B) Overexpression of AKAP8-wt and AKAP8-del in ovarian cancer cells was confirmed by western blot.

(C) IF assays showing the condensation of AKAP8-wt or AKAP8-del in OVCAR3 and SKOV3 cells. Scale bar, 10 μm.

(D and E) The ability of the AKAP8 101–210 region in promoting ovarian cancer cells' proliferation was examined by colony formation and CCK-8 assays.

(F and G) Representative image of migration and invasion of ovarian cancer cells with AKAP8-wt and AKAP8-del overexpression. Scale bar, 200μm.

(H) RT-PCR analysis of hnRNPUL1-L or S expression in ovarian cancer cells with AKAP8-wt or AKAP8-del overexpression.

(I) Representative western blot of hnRNPUL1 protein levels in ovarian cancer cells transfected with AKAP8-wt and AKAP8-del (left) and relative grayscale protein value (right).

(J) Relative luciferase activity of cells with AKAP8-wt or AKAP8-del, and pGL3-hnRNPUL1-S, pGL3-hnRNPUL1-Delete as well as pGL3-hnRNPUL1-L. Data were shown as mean ± SD from three independent experiments. *$p < 0.05$, **$p < 0.01$, ns, not significant.

AKAP8 phase separation contributes to ovarian cancer progression

AKAP8 was demonstrated to phase separate in triple-negative breast cancer cells, and its 101–210 region is essential for condensation.[20] To explore the implication of AKAP8 phase separation in its role of promoting ovarian cancer, we over-expressed wide-type AKAP8 or its mutant depleting 101–210 region (Δ101-210) and detected the protein expression by western blot (Figures 4A and 4B) in OVCAR3 and SKOV3 Cells. Immunofluorescence staining assays showed that both wide-type AKAP8 and mutated AKAP8 were mainly distributed in the nucleus, though

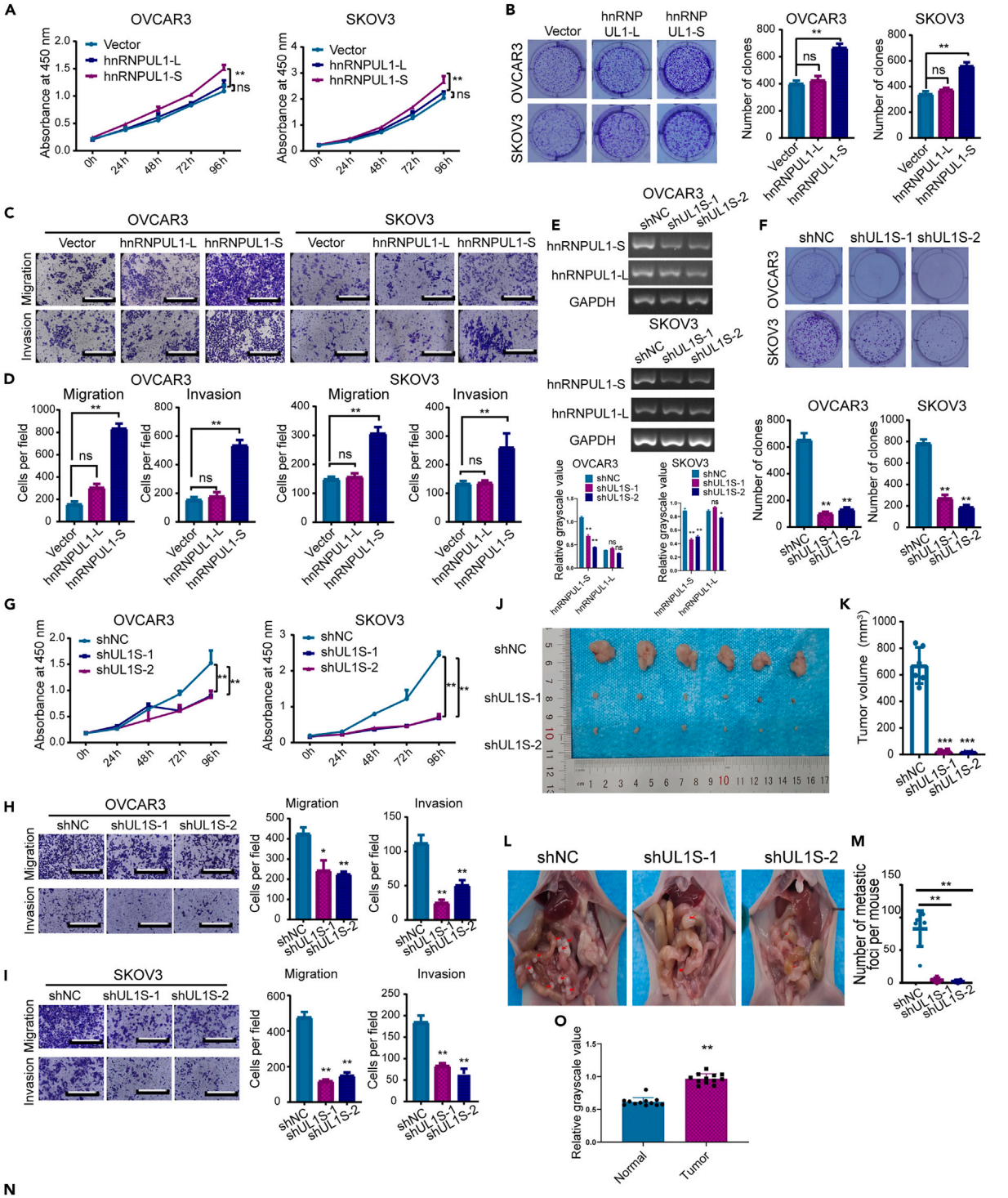
A
OVCAR3
SKOV3
Absorbance at 450 nm
Vector
hnRNPUL1-L
hnRNPUL1-S
0h
24h
48h
72h
96h
**
ns
B
Vector
hnRNP UL1-L
hnRNP UL1-S
OVCAR3
SKOV3
Number of clones
C
Migration
Invasion
D
Cells per field
E
shNC
shUL1S-1
shUL1S-2
GAPDH
Relative grayscale value
F
G
H
I
J
K
Tumor volume (mm³)
L
M
Number of metastic foci per mouse
O
Normal
Tumor
N
N1 T1 N2 T2 N3 T3 N4 T4 N5 T5 N6 T6 N7 T7 N8 T8 N9 T9 N10 T10 N11 T11 N12 T12

Figure 5. hnRNPUL1-S facilitates the proliferation and metastasis of ovarian cancer cells

(A) Proliferation of ovarian cancer cells over-expressing hnRNPUL1-S, hnRNPUL1-L, or empty vector was determined by CCK-8 assays.

(B) Colony formation assays of ovarian cancer cells over-expressing hnRNPUL1-S, hnRNPUL1-L, or empty vector.

(C) Representative images of transwell assay showing the migration and invasion abilities of ovarian cancer cells over-expressing hnRNPUL1-S, hnRNPUL1-L, or empty vector.

(D) Corresponding statistics of migrated and invaded cells are shown. Scale bar, 200 μm.

(E) Representative RT-PCR detecting hnRNPUL1-RNA expression in ovarian cancer cells with two independent shRNAs targeting hnRNPUL1 short isoform or shRNA-control (upper) and relative grayscale RNA value below).

(F) Colony formation assays of cell lines described in (E).

(G) Proliferation of OVCAR3 and SKOV3 cells as described in (E), was examined by CCK-8 assay.

(H and I) The migration and invasion abilities of OVCAR3 and SKOV3 cells (left) as described in (E) were examined by transwell assays, and corresponding statistics of migrated or invaded cells were shown at the (right). Scale bar, 200 μm.

(J) Tumor growth of xenograft derived from ovarian cancer cells upon hnRNPUL1 knockdown.

(K) Tumor weight for xenografts excised from (J).

(L) Representative images of peritoneal metastatic xenograft model.

(M) The number of ovarian metastasis derived from cells was described in (L).

(N) Representative hnRNPUL1-S RNA level in fresh ovarian tumor samples and adjacent normal samples by RT-PCR.

(O) Relative grayscale of hnRNPUL1-S RNA value. Data were shown as mean ± SD from three independent experiments. $^{**}p < 0.01$, $^{***}p < 0.001$, ns, not significant.

a marginal portion of mutated AKAP8 was found in the cytoplasm (Figure 4C). However, wide-type AKAP8 but not it's mutant formed nucleic puncta in ovarian cancer cells, demonstrating that AKAP8 phase separated through the 101–210 region (Figure 4C). Then we assessed the effect of AKAP8 condensation on its oncogenic role in ovarian cancer cells. Colony formation and CCK-8 assays revealed that overexpression of AKAP8 (Δ101-210) exerted a negligible effect on cell proliferation compared with that wide-type AKAP8 promoted cell proliferation substantially (Figures 4D and 4E). A similar effect was also found on migration and invasion of ovarian cells (Figures 4F and 4G), suggesting that AKAP8 phase separation is required to promote ovarian cancer.

To confirm that AKAP8 condensation contributed to the malignancy of ovarian cancer through hnRNPUL1 regulation, we evaluated the effect of AKAP8 condensation on hnRNPUL1 expression. Real time-qPCR and western blot assays showed that AKAP8 promoted hnRNPUL1 expression, but depletion of AKAP8 phase separation disrupted this effect (Figures 4H and 4I). ChIP assays also revealed that loss of AKAP8 phase separation decreased its binding at the hnRNPUL1 promoter compared with wide-type AKAP8 (Figure S4). In addition, AKAP8 (Δ101-210) failed to promote the luciferase activity in cells transfected with neither hnRNPUL1-S nor hnRNPUL1-S-Delete and hnRNPUL1-L (Figure 4J). These data indicate that AKAP8 phase separation is indispensable for regulating the expression of hnRNPUL1 in ovarian cancer.

hnRNPUL1 acts as an oncogenic driver in ovarian cancer

To assess the role of hnRNPUL1 in ovarian cancer, we first analyzed the expression of hnRNPUL1 protein expression level according to GEO and CPTAC databases. In contrast to normal ovarian epithelial cells, we observed that hnRNPUL1 was up-regulated in ovarian cancer cells (Figures S5A and S5B). Next, the effect of hnRNPUL1 on ovarian cancer patients' survival was analyzed. According to a Kaplan-Meier survival analysis, patients with high hnRNPUL1 expression exhibited significantly shorter overall survival times than patients with low hnRNPUL1 expression (Figure S5C), suggesting that elevated hnRNPUL1 expression predicts a worse prognosis for ovarian cancer patients.

Next, we sought to confirm whether hnRNPUL1 could be a promoter of ovarian cancer. We generated OVCAR3 and SKOV3 cell lines with stable overexpression of hnRNPUL1-S or hnRNPUL1-L, respectively. Western blot showed that when hnRNPUL1-S was over-expressed in OVCAR3 and SKOV3 cells in comparison to hnRNPUL1-L overexpression and the control groups, the levels of hnRNPUL1-S protein were found to be higher (Figure S5D). CCK-8 assays revealed that ectopic expression of hnRNPUL1-S significantly promoted the proliferation of ovarian cancer cells, while hnRNPUL1-L overexpression had no such effect compared with the control groups (Figure 5A). Consistently, hnRNPUL1-S but not hnRNPUL1-L strongly enhanced the colony formation ability of ovarian cancer cells compared with the control group (Figure 5B). Moreover, transwell assays revealed a stronger migration ability of the OVCAR3 and SKOV3 cells over-expressing hnRNPUL1-S compared with the OVCAR3 and SKOV3 cells with either hnRNPUL1-L or empty vector (Figures 5C and 5D).

To further examine the role of the hnRNPUL1-S isoform in ovarian cancer, we analyzed the cellular phenotype changes following hnRNPUL1-S knockdown in both OVCAR3 and SKOV3 cells. These alterations included cell proliferation, colony formation capacity, migration, and invasion. In comparison to control cells. PCR and western blot analysis showed that the expression of hnRNPUL1 significantly decreased in OVCAR3 and SKOV3 cells (Figures 5E and S5E). However, specific knockdown of hnRNPUL1-S had little effect on the expression hnRNPUL1-L (Figure 5E). When hnRNPUL1-S was knocked down in ovarian cancer cell lines compared to control cells, cell proliferation, and colony formation capacity were significantly decreased (Figures 5F and 5G). Meanwhile, depletion of hnRNPUL1-S also inhibited the invasion and migration of ovarian cancer cells (Figures 5H and 5I). Next, we examined the role of hnRNPUL1-S in tumorigenesis and metastasis using *in vivo* xenografts models. Ovarian cancer cells with stable knockdown of hnRNPUL1-S or with control were independently injected into nude mice. We found that the xenografts with hnRNPUL1-S knockdown exhibited an obvious size and tumor weight reduction compared with the control group (Figures 5J and 5K). A decreased metastasis rate in the hnRNPUL1-S knockdown groups compared with the control group was also observed (Figures 5L and 5M).

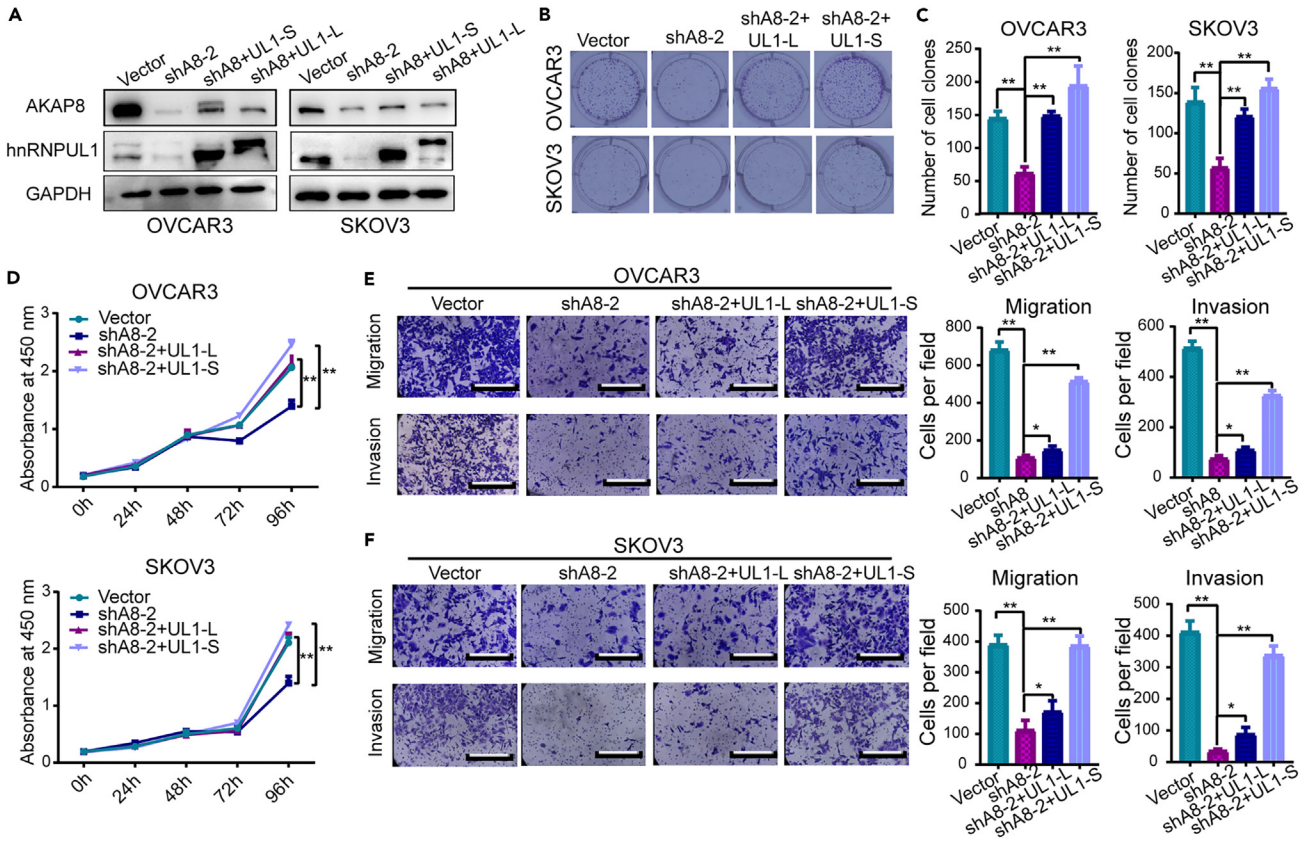

Figure 6. Ectopic expression of hnRNPUL1-S ameliorates the tumor suppressive effect of AKAP8 deficiency in ovarian cancer cells

(A) Western blot assay confirmed hnRNPUL1-S or hnRNPUL1-L overexpression in AKAP8 knocking down ovarian cancer cells.

(B) Colony formation assays of ovarian cancer cells as described in (A).

(C) The quantification of colony number from (B).

(D Proliferation of ovarian cancer cells as described in (A).

(E and F) The migration and invasion ability of ovarian cancer cells as described in (A) Scale bar, 200 μm. Data were shown as mean ± SD from three independent experiments. *$p < 0.05$, **$p < 0.01$.

In addition, we examined the mRNA expression of hnRNPUL1-S in ovarian tumors and fallopian tube epithelium and observed that the hnRNPUL1-S mRNA level was significantly higher in ovarian tumors than in fallopian tube epithelium samples (Figure 5N). These results demonstrate that hnRNPUL1-S plays an oncogenic role in ovarian cancer.

Overexpression of hnRNPUL1 short isoform rescues the anti-tumorigenesis effects of AKAP8 knockdown

To test whether the ectopic expression of hnRNPUL1 could improve the tumor suppressive impact of AKAP8 deficiency on ovarian cancer, we first generated ovarian cancer cell lines with AKAP8 knockdown followed by overexpression of hnRNPUL1-S or hnRNPUL1-L. Western blot analysis revealed that overexpression of hnRNPUL1-S dramatically elevated the expression of AKAP8-depletion but partially elevated with overexpression of hnRNPUL1-L and empty vector (Figure 6A). After AKAP8 knockdown, hnRNPUL1-S overexpression effectively reversed this effect by restoring cell proliferation and colony formation ability, as demonstrated by CCK-8 and colony formation experiment (Figures 6B–6D). Cell migration and invasion that had been reduced by AKAP8 deficiency were significantly increased after hnRNPUL1-S overexpression, in contrast to hnRNPUL1-L over-expressed cells and empty vector (Figures 6E and 6F). These results indicate that hnRNPUL1-S is an important downstream AKAP8 target that promotes ovarian cancer.

Down-regulation of AKAP8 enhances PARPi sensitivity in ovarian cancer cells

Given that it has been shown that hnRNPUL1 controls the expression of PARP1 and that PARPis are emerging to be promising therapeutic candidates for the treatment of ovarian cancer,[7,8] we intended to find out if AKAP8-mediated hnRNPUL1 expression conferred PARPi insensitivity in ovarian cancer cells. Firstly, we detected PARP1 expression upon hnRNPUL1 knockdown by RT-qPCR. Results showed that AKAP8 inhibition decreased PARP1 expression at both RNA and protein levels (Figure 7A). Notably, hnRNPUL1-S overexpression but not hnRNPUL1-L could rescue the expression of PARP1, indicating AKAP8 could regulate PARP1 expression through hnRNPUL1 (Figures S6A

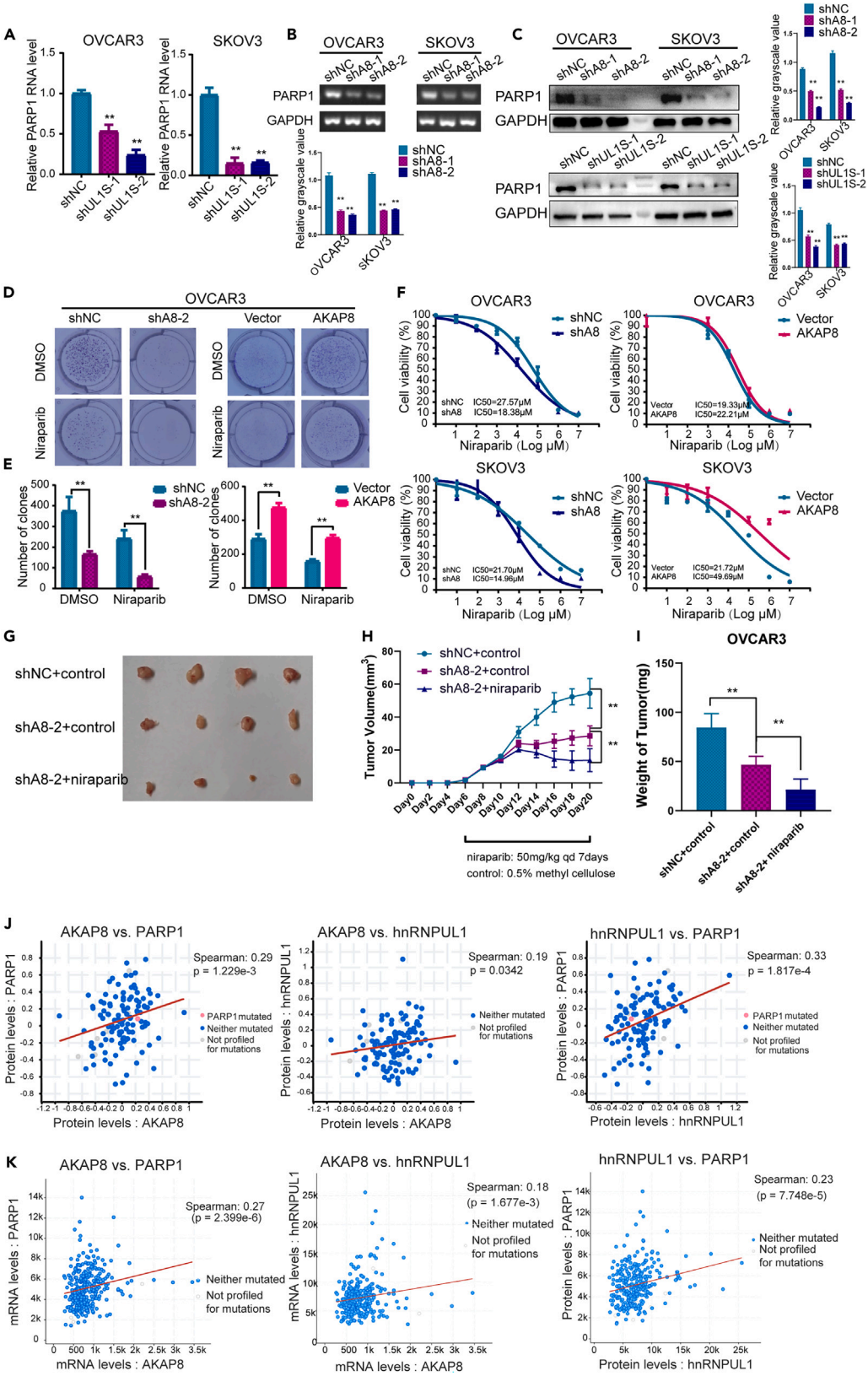
A
OVCAR3
SKOV3
Relative PARP1 RNA level
shNC
shUL1S-1
shUL1S-2
B
OVCAR3
SKOV3
shNC
shA8-1
shA8-2
PARP1
GAPDH
Relative grayscale value
C
OVCAR3
SKOV3
shNC
shA8-1
shA8-2
shUL1S-1
shUL1S-2
PARP1
GAPDH
Relative grayscale value
D
OVCAR3
shNC
shA8-2
Vector
AKAP8
DMSO
Niraparib
E
Number of clones
shNC
shA8-2
Vector
AKAP8
DMSO
Niraparib
F
OVCAR3
SKOV3
shNC
shA8
Vector
AKAP8
Cell viability (%)
Niraparib (Log μM)
shNC IC50=27.57μM
shA8 IC50=18.38μM
Vector IC50=19.33μM
AKAP8 IC50=22.21μM
shNC IC50=21.70μM
shA8 IC50=14.96μM
Vector IC50=21.72μM
AKAP8 IC50=49.69μM
G
shNC+control
shA8-2+control
shA8-2+niraparib
H
shNC+control
shA8-2+control
shA8-2+niraparib
Tumor Volume(mm3)
Day0
Day2
Day4
Day6
Day8
Day10
Day12
Day14
Day16
Day18
Day20
niraparib: 50mg/kg qd 7days
control: 0.5% methyl cellulose
I
OVCAR3
Weight of Tumor(mg)
shNC+control
shA8-2+control
shA8-2+niraparib
J
AKAP8 vs. PARP1
Spearman: 0.29
p = 1.229e-3
AKAP8 vs. hnRNPUL1
Spearman: 0.19
p = 0.0342
hnRNPUL1 vs. PARP1
Spearman: 0.33
p = 1.817e-4
Protein levels : PARP1
Protein levels : hnRNPUL1
Protein levels : AKAP8
PARP1 mutated
Neither mutated
Not profiled for mutations
K
AKAP8 vs. PARP1
Spearman: 0.27
(p = 2.399e-6)
AKAP8 vs. hnRNPUL1
Spearman: 0.18
(p = 1.677e-3)
hnRNPUL1 vs. PARP1
Spearman: 0.23
(p = 7.748e-5)
mRNA levels : PARP1
mRNA levels : hnRNPUL1
mRNA levels : AKAP8
Protein levels : PARP1
Protein levels : hnRNPUL1
Neither mutated
Not profiled for mutations

Figure 7. AKAP8 up-regulation decreases niraparib sensitivity in ovarian cancer cells

(A) RT-qPCR analysis of relative PARP-1 RNA level after hnRNPUL1 knockdown in ovarian cancer cells.

(B) RT-PCR analysis of PARP-1 RNA level after AKAP8 knockdown in ovarian cancer cells.

(C) Representative western blot of PARP-1 protein expression upon AKAP8 or hnRNPUL1 knockdown in ovarian cancer cells (left) and relative protein expression (right).

(D and E) Cell viability of AKAP8 over-expressing or knocking down ovarian cancer cells in the presence of niraparib or DMSO was determined by colony formation assays. Scale bar, 200 μm.

(F) Cell viability of AKAP8 over-expressing or knocking down ovarian cancer cells treated with different concentrations of niraparib was detected by CCK-8 assays.

(G) Representative images of tumorigenesis xenograft model using mice injected with OVCAR3 cells niraparib or control.

(H and I) Tumor volume and tumor weight for xenograft excised from (G).

(J and K) Pearson correlation analysis between AKAP8, hnRNPUL1,and PARP-1, respectively, at AKAP8 Protein expression level (Ovarian cancer database from TCGA Pan Cancer, mass spectrometry by CPTAC/174 samples), and mRNA expression level(Ovarian cancer database from TCGA Pan Cancer, RNA Seq V2 RSEM/307 samples). Data were shown as mean ± SD from three independent experiments. $^{**}p < 0.01$.

and S6B). Conversely, AKAP8 knockdown also substantially suppressed PARP1 RNA expression (Figure 7B). Western blot assays revealed that either AKAP8 or hnRNPUL1 knockdown decreased PARP1 expression (Figure 7C). To further confirm the effect of AKAP8 on PARP inhibitor sensitivity in ovarian cancer cells, niraparib, a PARP inhibitor, was used to treat ovarian cancer cells with AKAP8 knockdown or overexpression, and then cell viability and IC50 of niraparib were detected. As shown in Figures 7D and 7E, AKAP8 knockdown significantly aggravated the decrease of the colony formation ability by niraparib treatment. Conversely, overexpression of AKAP8 ameliorated the suppressive effect of niraparib on ovarian cancer cells' ability to form colonies (Figures 7D and 7E). Consistently, ovarian cancer cells with AKAP8 knockdown showed more sensitivity to niraparib treatment compared with the control cells, whereas overexpression of AKAP8 decreased niraparib cytotoxicity in ovarian cancer cells with higher IC50 values (Figure 7F).

In addition, we took advantage of the tumor xenograft model to confirm the effects of niraparib in the progression tumor of ovarian cancer *in vivo* (Figures 7G–7I). As shown in (Figures 7H and 7I), niraparib suppress the progression tumor of ovarian cancer *in vivo*. In mice with niraparib compared to control mice, the tumor growth and the average tumor volume were significantly smaller (Figures 7H and 7I).

We finally analyzed the correlations between AKAP8, hnRNPUL1, and PARP1 expression both at protein level and mRNA level in clinical samples of ovarian cancer (Figures 7J and 7K), respectively. hnRNPUL1 and PARP1 expression were positively correlated with AKAP8 expression at protein level, and PARP1 and hnRNPUL1 expression were likewise positively correlated (Figure 7J). Similar result was observed at mRNA level (Figure 7K). Collectively, the results suggest that AKAP8 up-regulation contributes to niraparib insensitivity in ovarian cancer cells.

DISCUSSION

AKAP8 was recently reported to be implicated in several cancers including breast cancer,[15,16] colorectal cancer,[17,18] cervical cancer,[13] and lung cancer.[19] Although these studies have shown that AKAP8 promotes tumorigenesis, another study has reported that AKAP8 acts as a tumor suppressor gene in triple-negative breast cancer.[15] In this study, we show that AKAP8 plays an oncogenic role in ovarian cancer by regulating ovarian cancer cell proliferation both *in vitro* and *in vivo*.

AKAP8 was initially found as A-kinase anchoring protein that attracts protein kinase A to chromatin and nuclear structures,[12,21] Additional studies revealed that it also serves as a DNA-binding protein and an RNA-binding protein.[14,22] As a highly abundant nucleic protein, AKAP8 can modulate the activity of splicing factors, thus regulating pre-mRNA splicing.[13] AKAP8 can also regulate Pol II and H3K4me3 enrichment at the chromatin.[14]

In our study, we performed RNA-seq upon AKAP8 knockdown in ovarian cancer cells and found its different effect on two hnRNPUL1 isoforms (hnRNPUL1-L and hnRNPUL1-S) resulting from differential first exon usages at 5′ end of hnRNPUL1 mRNA. AKAP8 eCLIP assays showed AKAP8 didn't interact with hnRNPUL1 mRNA. However, AKAP8 was mainly localized in the nucleus and enriched in chromatin in ovarian cancer cells. ChIP assays showed that AKAP8 bound to the hnRNPUL1 promoter but AKAP8 regulated the hnRNPUL1-S isoform expression. We have provided evidence that AKAP8 mediated the transcriptional regulation of hnRNPUL1. Consistently, by performing Pol II and H3K4me3 ChIP assays, we found that AKAP8 knockdown decreased the enrichment of H3K4me3 and Pol II at hnRNPUL1 promoter in ovarian cancer cells.

Transcriptional factors, chromatin regulators, and essential elements of the basic transcriptional machinery interact to control transcription. Wang and collaborators reveal that the interactions between transcription factor-bound distal enhancers and their target genes are made easier by the presence of CTCF binding sites at chromatin domain boundaries.[23] Recently, CTCF has been identified as a DNA-binding protein with crucial roles in chromatin topological structure maintenance and DNA looping induction. Other transcription factors can influence cancer-specific CTCF binding to regulate oncogenic gene expression.[24] Considering that, we have further identified and functionally characterized a novel transcription factor associated with AKAP8 to regulate hnRNPUL1 expression. We revealed after AKAP8 knockdown, the enrichment of CTCF at the hnRNPUL1-S promoter was down-regulated. By performing the luciferase activity reporter assays, we observed that overexpression of AKAP8 could enhance the luciferase activity in ovarian cancer cells transfected with pGL3-hnRNPUL1-S, but not pGL3-hnRNPUL1-S-Delete or pGL3-hnRNPUL1-L. Together, these data suggest that AKAP8 regulates the specific hnRNPUL1 isoform transcription.

Phase separation influences the expression of certain genes by promoting particular mutations that lead to cancer, and AKAP8 phase separation has a link with chromosomal transcription and RNA splicing.[12,14] In the present study, we provided a global view and mechanistic insights into the impact of AKAP8 phase separation on ovarian cancer progression, demonstrating the biological role of AKAP8 phase

separation. Notably, disruption of AKAP8 phase separation suppressed its function of regulating the transcription of hnRNPUL1 specific isoform. We revealed that hnRNPUL1-S was over-expressed in ovarian cancer, suggesting that hnRNPUL1-S might be essential for the prognosis and treatment of ovarian cancer. We also noted that the overexpression of hnRNPUL1-S rescued the anti-tumorigenesis effects of AKAP8 knockdown. These findings provide new light on the development of clinical biomarkers and therapeutic approaches focusing on AKAP8 and hnRNPUL1.

It has been reported that hnRNPUL1 controls PARP1 expression. In a wide range of ovarian cancer patients, PARP inhibitors are helpful.[25,26] However, resistance brought on by reduced expression of the therapeutic target PARP-1 needs to be clinically assessed. In contemporary clinical practice, patients who test positive for genetic mutations in genes encoding DNA repair proteins that cause homologous recombination deficiency (HRD), particularly mutations in breast and ovarian cancer, are frequently chosen for PARPi therapy.[7,27] The PARPis are the first clinically authorized medication capable of inducing "synthetic lethality" in patients with HRD tumors.[27,28] Although efforts have been made, the mechanisms underlying PARPis resistance and viable therapeutic techniques to overcome these processes of resistance remain elusive, and long-term survival rates for patients with ovarian cancer remain to be unsatisfactory, which represents a therapeutic challenge. We demonstrated that the down-regulation of AKAP8 enhanced niraparib cytotoxicity in ovarian cancer cells. Our study implied that AKAP8-mediated hnRNPUL1 expression played a crucial role in ovarian cancer progression and PARP inhibitor sensitivity.

In conclusion, our present study demonstrated that AKAP8 promoted ovarian cancer progression and attenuated PARP inhibitor sensitivity by regulating the isoform-specific hnRNPUL1 transcription. We also clarified the oncogenic role of AKAP8 phase separation and revealed a new activity of AKAP8 in ovarian cancer. Therefore, AKAP8 could be useful as a potential therapeutic target for ovarian cancer.

Limitations of the study

Although the current study characterizes AKAP8-RNA binding protein in ovarian cancer using several innovative technologies. There are still some limitations to our study that need to be mentioned. First, the study identified potential AKAP8 targets and partially characterized one of these targets (hnRNPUL1). Secondly, the study provides novel information regarding the molecular activity of AKAP8. However, the critical molecular role of AKAP8 in ovarian cancer function is still incomplete. It would be better in the future to make up further experiments like chIP sequencing analysis and then provide a candidate AKAP8 consensus binding motif. Besides, we demonstrated the oncogenic role of AKAP8 phase separation and revealed a new activity of AKAP8 in ovarian cancer progression, it remains the tumorigenesis effect validation of AKAP8 (101–210) domain in animal models, and the verification of the precise or other biological effects. Finally, we showed that the down-regulation of AKAP8 enhances the sensitivity of ovarian cancer cells to niraparib (a PARP inhibitor). In the future, we will continue to explore other classes of PARP inhibitors. This would reflect a much stronger clinical value.

STAR★METHODS

Detailed methods are provided in the online version of this paper and include the following:

- KEY RESOURCES TABLE
- RESOURCE AVAILABILITY
  - Lead contact
  - Materials availability
  - Data and code availability
- EXPERIMENTAL MODEL AND STUDY PARTICIPANT DETAILS
  - Cell lines and cell culture
  - Clinical samples
  - Tumor xenografts in nude mice
- METHOD DETAILS
  - Plasmid construction
  - *In vivo* tumorigenesis and metastasis assays
  - *In vivo* tumorigenesis drug treatment
  - Cell transfection
  - Lentiviruses
  - Western blot
  - Cell proliferation assay
  - Transwell migration and invasion assays
  - RNA extraction and RT-PCR
  - Immunofluorescence and confocal microscopy
  - Nuclear and cytoplasmic separation
  - Immunoprecipitation (IP) and RNA immunoprecipitation (RIP)
  - RNA-seq and data analysis
  - Enhanced crosslinking immunoprecipitation followed by sequencing (eCLIP-seq)
  - Chromatin immunoprecipitation (ChIP) assay

- Dual-luciferase reporter assay
- QUANTIFICATION AND STATISTICAL ANALYSIS

SUPPLEMENTAL INFORMATION

Supplemental information can be found online at https://doi.org/10.1016/j.isci.2024.109744.

ACKNOWLEDGMENTS

We are grateful to the laboratory members for their helpful and inspiring discussions. We thank the Clinical Research Center of the Third Affiliated Hospital of Chongqing Medical University of China for providing us a good lab environment for our experiment. We also appreciate the excellent cooperation of our colleagues in the Obstetrics and Gynecology Department of the Third Affiliated Hospital of Chongqing Medical University of China. We thank the Biochemistry Department of the Faculty of Sciences of the University of Douala-Cameroon for their assistance. We would like to thank the Institute of Biology and Molecular Medicine of the Université Libre de Bruxelles-Belgium for their guidance. This work was supported by grants from The National Natural Science Foundation of China (No. 32101164 to Y.Y. and No. 82072886 to P.Y.) and the Natural Science Foundation of Chongqing, China (No. CSTB2022NSCQ-MSX0897 to T.L.).

AUTHOR CONTRIBUTIONS

P.Y. and T.L. designed the study and provided guidance on interpreting the results. Y.M. and H.C.W. carried out the experiments, collected the data, and analyzed the result. W.Q.L. performed data collection and statistical analysis. D.Y., X.Y.L., and Y.Y. participated in the clinical specimen detection. H.Y.Z. helped with animal assays, acquired and assembled clinical information and tumor data. Y.M. drafted the manuscript. J.X., A.N.N., and J.S. revised the manuscript. P.Y. and T.L. edited the manuscript. All the authors read and approved the final manuscript.

DECLARATION OF INTERESTS

The authors declare no competing interests.

Received: July 11, 2023
Revised: December 8, 2023
Accepted: April 11, 2024
Published: April 16, 2024

REFERENCES

1. Bray, F., Ferlay, J., Soerjomataram, I., Siegel, R.L., Torre, L.A., and Jemal, A. (2018). Global cancer statistics 2018: GLOBOCAN estimates of incidence and mortality worldwide for 36 cancers in 185 countries. CA A Cancer J. Clin. *68*, 394–424.
2. Islami, F., Torre, L.A., Drope, J.M., Ward, E.M., and Jemal, A. (2017). Global cancer in women: cancer control priorities. Cancer Epidemiol. Biomarkers Prev. *26*, 458–470.
3. Herzog, T.J. (2006). The current treatment of recurrent ovarian cancer. Curr. Oncol. Rep. *8*, 448–454.
4. Ait Saada, A., Lambert, S.A.E., and Carr, A.M. (2018). Preserving replication fork integrity and competence via the homologous recombination pathway. DNA Repair *71*, 135–147.
5. González-Martín, A., Pothuri, B., Vergote, I., DePont Christensen, R., Graybill, W., Mirza, M.R., McCormick, C., Lorusso, D., Hoskins, P., Freyer, G., et al. (2019). Niraparib in Patients with Newly Diagnosed Advanced Ovarian Cancer. N. Engl. J. Med. *381*, 2391–2402.
6. Mirza, M.R., Monk, B.J., Herrstedt, J., Oza, A.M., Mahner, S., Redondo, A., Fabbro, M., Ledermann, J.A., Lorusso, D., Vergote, I., et al. (2016). Niraparib Maintenance Therapy in Platinum-Sensitive, Recurrent Ovarian Cancer. N. Engl. J. Med. *375*, 2154–2164.
7. Shao, F., Liu, J., Duan, Y., Li, L., Liu, L., Zhang, C., and He, S. (2020). Efficacy and safety of PARP inhibitors as the maintenance therapy in ovarian cancer: a meta-analysis of nine randomized controlled trials. Biosci. Rep. *40*, BSR20192226.
8. Gralewska, P., Gajek, A., Marczak, A., Mikuła, M., Ostrowski, J., Śliwińska, A., and Rogalska, A. (2020). PARP Inhibition Increases the Reliance on ATR/CHK1 Checkpoint Signaling Leading to Synthetic Lethality-An Alternative Treatment Strategy for Epithelial Ovarian Cancer Cells Independent from HR Effectiveness. Int. J. Mol. Sci. *21*, 9715.
9. Eide, T., Coghlan, V., Orstavik, S., Holsve, C., Solberg, R., Skålhegg, B.S., Lamb, N.J., Langeberg, L., Fernandez, A., Scott, J.D., et al. (1998). Molecular cloning, chromosomal localization, and cell cycle-dependent subcellular distribution of the A-kinase anchoring protein, AKAP95. Exp. Cell Res. *238*, 305–316.
10. Deng, Z., Liu, R., Guo, H., Yao, L., Ruan, F., Wang, K., Qiu, G., Luo, Z., Luo, G., and Guo, D. (2020). AKAP95 Transports Cx43 into Nucleus, Regulating G1/S Transition of A549 Cells.
11. Landsverk, H.B., Carlson, C.R., Steen, R.L., Vossebein, L., Herberg, F.W., Taskén, K., and Collas, P. (2001). Regulation of anchoring of the RIIalpha regulatory subunit of PKA to AKAP95 by threonine phosphorylation of RIIalpha: implications for chromosome dynamics at mitosis. J. Cell Sci. *114*, 3255–3264.
12. Eide, T., Carlson, C., Taskén, K.A., Hirano, T., Taskén, K., and Collas, P. (2002). Distinct but overlapping domains of AKAP95 are implicated in chromosome condensation and condensin targeting. EMBO Rep. *3*, 426–432.
13. Hu, J., Khodadadi-Jamayran, A., Mao, M., Shah, K., Yang, Z., Nasim, M.T., Wang, Z., and Jiang, H. (2016). AKAP95 regulates splicing through scaffolding RNAs and RNA processing factors. Nat. Commun. *7*, 13347.
14. Jiang, H., Lu, X., Shimada, M., Dou, Y., Tang, Z., and Roeder, R.G. (2013). Regulation of transcription by the MLL2 complex and MLL complex-associated AKAP95. Nat. Struct. Mol. Biol. *20*, 1156–1163.
15. Hu, X., Harvey, S.E., Zheng, R., Lyu, J., Grzeskowiak, C.L., Powell, E., Piwnica-Worms, H., Scott, K.L., and Cheng, C. (2020). The RNA-binding protein AKAP8 suppresses tumor metastasis by antagonizing EMT-associated alternative splicing. Nat. Commun. *11*, 486.
16. Huang, P., Sun, Q., Zhuang, W., Peng, K., Wang, D., Yao, Y., Guo, D., Zhang, L., Shen, C., Sun, M., et al. (2017). Epac1, PDE4, and PKC protein expression and their association with AKAP95, Cx43, and cyclinD2/E1 in breast cancer tissues. Thorac. Cancer *8*, 495–500.
17. Yang, M.H., Hu, Z.Y., Xu, C., Xie, L.Y., Wang, X.Y., Chen, S.Y., and Li, Z.G. (2015). MALAT1 promotes colorectal cancer cell proliferation/migration/invasion via PRKA kinase anchor

protein 9. Biochim. Biophys. Acta *1852*, 166–174.

18. Hu, Z.Y., Wang, X.Y., Guo, W.B., Xie, L.Y., Huang, Y.Q., Liu, Y.P., Xiao, L.W., Li, S.N., Zhu, H.F., Li, Z.G., and Kan, H. (2016). Long non-coding RNA MALAT1 increases AKAP-9 expression by promoting SRPK1-catalyzed SRSF1 phosphorylation in colorectal cancer cells. Oncotarget *7*, 11733–11743.
19. Chen, R., Chen, Y., Yuan, Y., Zou, X., Sun, Q., Lin, H., Chen, X., Liu, M., Deng, Z., Yao, Y., et al. (2020). Cx43 and AKAP95 regulate G1/S conversion by competitively binding to cyclin E1/E2 in lung cancer cells. Thorac. Cancer *11*, 1594–1602.
20. Li, W., Hu, J., Shi, B., Palomba, F., Digman, M.A., Gratton, E., and Jiang, H. (2020). Biophysical properties of AKAP95 protein condensates regulate splicing and tumorigenesis. Nat. Cell Biol. *22*, 960–972.
21. Kubota, S., Morii, M., Yuki, R., Yamaguchi, N., Yamaguchi, H., Aoyama, K., Kuga, T., Tomonaga, T., and Yamaguchi, N. (2015). Role for Tyrosine Phosphorylation of A-kinase Anchoring Protein 8 (AKAP8) in Its Dissociation from Chromatin and the Nuclear Matrix. J. Biol. Chem. *290*, 10891–10904.
22. Marstad, A., Landsverk, O.J.B., Strømme, O., Otterlei, M., Collas, P., Sundan, A., and Brede, G. (2016). A-kinase anchoring protein AKAP95 is a novel regulator of ribosomal RNA synthesis. FEBS J. *283*, 757–770.
23. Wang, H., Zang, C., Taing, L., Arnett, K.L., Wong, Y.J., Pear, W.S., Blacklow, S.C., Liu, X.S., and Aster, J.C. (2014). NOTCH1-RBPJ complexes drive target gene expression through dynamic interactions with superenhancers. Proc. Natl. Acad. Sci. USA *111*, 705–710.
24. Fang, C., Wang, Z., Han, C., Safgren, S.L., Helmin, K.A., Adelman, E.R., Serafin, V., Basso, G., Eagen, K.P., Gaspar-Maia, A., et al. (2020). Cancer-specific CTCF binding facilitates oncogenic transcriptional dysregulation. Genome Biol. *21*, 247.
25. Konstantinopoulos, P.A., Ceccaldi, R., Shapiro, G.I., and D'Andrea, A.D. (2015). Homologous Recombination Deficiency: Exploiting the Fundamental Vulnerability of Ovarian Cancer. Cancer Discov. *5*, 1137–1154.
26. Makvandi, M., Pantel, A., Schwartz, L., Schubert, E., Xu, K., Hsieh, C.J., Hou, C., Kim, H., Weng, C.C., Winters, H., et al. (2018). A PET imaging agent for evaluating PARP-1 expression in ovarian cancer. J. Clin. Invest. *128*, 2116–2126.
27. Lord, C.J., and Ashworth, A. (2017). PARP inhibitors: Synthetic lethality in the clinic. Science *355*, 1152–1158.
28. González-Martín, A., Pothuri, B., Vergote, I., DePont Christensen, R., Graybill, W., Mirza, M.R., McCormick, C., Lorusso, D., Hoskins, P., Freyer, G., et al. (2019). Niraparib in patients with newly diagnosed advanced ovarian cancer. N. Engl. J. Med. *381*, 2391–2402.
29. Van Nostrand, E.L., Pratt, G.A., Shishkin, A.A., Gelboin-Burkhart, C., Fang, M.Y., Sundararaman, B., Blue, S.M., Nguyen, T.B., Surka, C., Elkins, K., et al. (2016). Robust transcriptome-wide discovery of RNA-binding protein binding sites with enhanced CLIP (eCLIP). Nat. Methods *13*, 508–514.
30. Anders, S., Reyes, A., and Huber, W. (2012). Detecting differential usage of exons from RNA-seq data. Genome Res. *22*, 2008–2017.

STAR★METHODS

KEY RESOURCES TABLE

REAGENT or RESOURCE	SOURCE	IDENTIFIER
Biological sample		
Peritoneal metastasis model and xenograft tumor models	Female immunodeficient nude mice (4 to 6 weeks old)	N/A
Antibodies		
anti-AKAP8	Abcam	ab72196
anti-hnRNPUL1	Affinity	DF781
anti-Flag M2	Sigma	F3165
anti-GAPDH	Proteintech	10494-1-AP
anti-snRNP70	Thermo Fisher,	PA5-110406
anti-PARP-1	Santa Cruz Biotechnology	SB-8007
anti-tubulin	Proteintech	11224-1-AP,
HRP-conjugated anti-mouse IgG	Proteintech	SA00001-1
HRP-conjugated anti-rabbit IgG	Proteintech	SA00001-2
anti-CTCF	Abcam	ab128873
anti-H3K4me3	Abcam	ab213224
anti-Poly II	Cell Signaling Technology	CST
Oligonucleotides		
Primer for RT-PCR and RT-qPCR assay	Sangon	Table S1
Primer for Chip-qPCR assay	Sangon	Table S1
Plasmids	Vigene	N/A
Penter/AKAP8	Vigene	N/A
shRNA (see Table S1)	Tsingke and Sangon	Table S1
Packaging vectors psPAX2and pMD2.G	Addgene	#12260 and #12259
Bacteria and virus strains		
TOP10 competent cell	Tsingke	TSC-C12
STBL3 competent cell	Tsingke	TSC-C06
BshT1	Thermo Fischer Scientific	91250250
EcorRI	Thermo Fischer Scientific	#FD0274
T4DNA Ligase	Biolabs	BO202A
PLKO.1	Addgene	#1864
Chemicals, peptides, and recombinant proteins		
Polybrene Infection/tansfection reagent	JetPRIME-Polyplus	101000046
Lipofectamine^{tm} transfection reagent	Thermo Fischer Scientific	L30000001
RPMI 1640 Medium	Gibco	C11875500BT
DMEM Medium	Gibco	C11995500BT
Foetal Bovine Serum (FBS)	Gibco	C04001-050
Penicillin/Streptomycin	Gibco	15140-122
Niraparib(PARP-1)	TargetMol	Cat#1038915-60-4
Formaldehyde and crystal violet	Beyotime	C0121
Ampicillin	VWR	#7177-48-2

(*Continued on next page*)

Continued

REAGENT or RESOURCE	SOURCE	IDENTIFIER
Kanamycin	VWR	#80030-956
Puromycin	Sigma-Aldrich	#P8833
Critical commercial assays		
BCA Protein Assay kit	Solarbio	Cat#PC0020
TIANamp Genemic DNA kit	TIANGEN	Cat#DP-304-02
TIANprep Mini plasmid kit	TIANGEN	Cat#DP103-02
Trizol reagent	Invitrogen	Cat#15596018
Bio-rad Protein Assay kit II	Bio-rad	5000002
SYBR Green PCR Master Mix	Vazyme	#Q711
SuperScript First Strand cDNA system	Vazyme	#Q711-02-AA
Gel Extraction Kit	Omega	D2500-01
CCK8- Assay Kit	DOJONDO	K1018
eCLIP -sequencing Assay Kit	Life Technologies	NP0321BOX
Chip Enzymatic Chromatin IP Kit	Cell Signaling	Cat#91820:9003
Superscript III Reverse Transcriptase kit	Thermo Fisher Scientific	18080093
RNA sequencing library kit	Agilent Technologies	5067-1514
RNA sequencing Assay Kit	Applied biosystems (Thermo Fisher Scientific)	4336772
Luciferase reporter detection Kit	TransDetect	#FR201-02
Deposited data		
Ovarian cancer samples data	The Cancer Genome Atlas Research Network	https://www.cbioportal.org
RNA-seq and data	This paper	https://dataview.ncbi.nlm.nih.gov/object/PRJNA843486?archive=sra
eCLIP-seq and data	This paper	https://dataview.ncbi.nlm.nih.gov/object/PRJNA1093080?archive=sra
ChIP seq	The Encyclopedia of DNA Elements(ENCODE)	https://www.encodeproject.org/experiments/ENCSR279NEA/
GEO database	National Center for Biotechnology Information	https://www.ncbi.nlm.nih.gov/gds/?term=GSE18520 or GSE27651
CPTAC database	Clinical Proteomic Tumor Analysis Consortium (NCI)	https://proteomics.cancer.gov/programs/cptac
Kaplan-Meier	Kaplan-Meier Plotter database	https://kmplot.com/analysis/index.php?p=service&cancer=ovar
Software and algorithms		
Adobe Illustrator	Adobe	https://www.adobe.com/
GraphPad Prism	GraphPad Sofware	https://www.graphpad.com/
R	The R foundation	https://www.r-project.org/
ImageJ	Schneider et al.,2012	https://imagej.nih.gov/ij
TopHat (v2.0.13)	The Center for Computational Biology at Johns Hopkins University	https://ccb.jhu.edu/software/tophat/tutorial.shtml
HTSeq (v0.6.0)	Github	https://github.com/htseq/htseq
DEXseq	Github	https://github.com/vivekbhr/Subread_to_DEXSeq

RESOURCE AVAILABILITY

Lead contact

Further information and requests for resources and reagents should be directed to and will be fulfilled by the lead contact (yiping@cqmu.edu.cn).

Materials availability

This study did not generate new unique reagents and all materials in this study are commercially available. Plasmids and associated vector maps generated is this study are available upon request. Any additional analysis information for this work is available by request to the lead contact.

Data and code availability

Data from publicly archive datasets are available from cBioIPortal database, GEO database, CPTAC database for ovarian cancer samples data, and ENCODE database data for AKAP8 ChIP seq. These accession numbers for the data sets are also listed in the key resources table. RNA-seq and eCLIP-seq data has been uploaded to the NCBI public database, under the project accession code: PRJNA843486 (RNA-seq) and PRJNA1093080 (eCLIP-seq). The codes for RNA-seq, eCLIP-seq, and DEXseq are provided in detail in Supplementary protocol. Any additional information require to reanalyze the data reported in this paper is available from the lead contact upon request.

EXPERIMENTAL MODEL AND STUDY PARTICIPANT DETAILS

Cell lines and cell culture

Human cell lines HEK293T, OVCAR3, and SKOV3 cells were acquired from the National Infrastructure of Cell Line Resource (Beijing, China). OVACR3 cells were cultured in RPMI 1640 (Gibco) media, whereas HEK293T and SKOV3 cells were grown in Dulbecco's Modified Eagle media (DMEM) (Gibco). 10% Foetal Bovine Serum (FBS) and 1% Penicillin/Streptomycin (Gibco) were added to all media as supplements. All of the cells were maintained alive at 37°C in a cell culture incubator with 5% CO_2.

Clinical samples

Human subjects were involved in this study. From December 2022 to December 2023, 24 patients, aged to 28 to 70, with ovarian serous epithelial (OSE) and normal fallopian tube epithelium (FTE) (details in Table S1), who intended for surgical removal at the Gynecology Department of the Third Affiliated Hospital of Chongqing Medical University of China were included. All tumor samples were pathologically confirmed, and the principle of informed consent was strictly respected. All subjects gave informed consent. Fresh tumor samples from ovarian cancer patients and non-ovarian cancer patients were collected preserved by liquid nitrogen and then subjected to PCR and western blot analysis. The study conformed to the ethical guidelines of the 1975 Declaration of Helsinki and was approved by the Ethical Committee of the Third Affiliated Hospital of Chongqing Medical University of China (Ethical approval number for human participants: 2022-93).

Tumor xenografts in nude mice

Mice subjects were involved in this study. For the *in vivo* experiment, 4-6 week-old female immunodeficient nude mice (Balb/c) were obtained from Beijing Army Experimental Animal Center Co., Ltd. (Beijing, China) and held under specific pathogen-free conditions. Mice were housed in a ventilated cages and were allowed to acclimate for a minimum of 3 days prior to manipulation. All animal studies were approved by the Institutional Animal Care and Use Committee of Chongqing Medical University (Ethical approval number for animal participants: IACUC-CQMU-2023-0254), and carried out according to institutional guidelines for animal experimentation protocols (NIH publications Nos. 80-23, revised 1996).

METHOD DETAILS

Plasmid construction

Complementary sense and anti-sense oligonucleotides encoding shRNAs targeting AKAP8 and hnRNPUL1 were made and cloned into the pLKO.1 vector to knock down these two genes. The following are the shRNA sequences that were utilized:

shA8-1(F): 5′-CCGGGCCAAGATCAACCAGCGTTTG CTCGAGCAAACGCTGGTTGATCTTGGCTTTTTG -3′
shA8-1(R) :5′-AATTCAAAAAGCCAAGATCAACCAGCGTTTGCTCGAGCAAACGCTGGTTGATCTTGGC -3′
shA8-2(F) :5′-CCGGACGTCTTAGCAGAGGTGATTACTCGAGTAATCACCTCTGCTAAGACGTTTTTTG -3′
shA8-2(R):5′-AATTCAAAAAACGTCTTAGCAGAGGTGATTACTCGAGTAATCACCTCTGCTAAGACGT-3′
shUL1-1(F):5′-CCGGGCCGCTGGATGCGATCCTGGGCTCGAGCCCAGGATCGCATCCAGCGGCTTTTTG-3′
shUL1-1(R):5′-AATTCAAAAAGCCGCTGGATGCGATCCTGGGCTCGAGCCCAGGATCGCATCCAGCGGC-3′
shUL1-2(F) : 5′-CCGGGTTCTCCTATTTGGATGCCATCTCGAGATGGCATCCAAATAGGAGAACTTTTTG-3′
shUL1-2(R): 5′-AATTCAAAAAGTTCTCCTATTTGGATGCCATCTCGAGATGGCATCCAAATAGGAGAAC-3′

For AKAP8 over-expression, AKAP8 was cloned into pENTER (pENTER-AKAP8). AKAP8 (101-210) and AKAP8 (101-210) delete were synthesized, and cloned in pENTER. hnRNPUL1 long and short isoforms were cloned into pcDNA3.1 (pcDNA3.1-hnRNPUL1-L and pcDNA3.1-hnRNPUL1-S). pGL3-hnRNPUL1-S, pGL3-hnRNPUL1-S-Delete, and pGL3-hnRNPUL1-L with different promoter sequences were constructed.

The reference sequences for AKAP8 and hnRNPUL1 are as follows:

- Homo sapiens A-kinase anchoring protein 8(AKAP8); NCBI Reference Sequence for mRNA: NM_005858.4;NCBI Reference Sequence for protein: NP_005849.1.

- Homo sapiens heterogeneous nuclear ribonucleoprotein U like 1 (HNRNPUL1-L), transcript variant 1, NCBI Reference Sequence for mRNA: NM_007040.6. NCBI Reference Sequence for protein: NP_008971.2.
- Homo sapiens heterogeneous nuclear ribonucleoprotein U like 1 (HNRNPUL1-S), transcript variant 5, NCBI Reference Sequence for mRNA: NM_001301016.3; NCBI Reference Sequence for protein: NP_001287945.1.

In vivo tumorigenesis and metastasis assays

The peritoneal metastasis model and xenograft tumor models were established using female immunodeficient nude mice (Balb/c) that were 4 to 6 weeks old. All nude mice were kept in a SPF animal room, with 5 nude mice in each cage. OVCAR3 cells down-regulated with AKAP8 or hnRNPUL1 and sh-Control, were collected and resuspended in PBS supplemented with 10% of Matrigel. 5×10^6 cells were subcutaneously injected into a mouse's posterior flank on one side for the tumorigenesis assay. Using a slide caliper to measure the tumor's size every five days, the tumor's volume was estimated as follows: volume = $(D\times d^2)/2$, where "D" meant the diameter with the longest length and "d" meant the diameter with the shortest length. 10^6 cells were injected into the peritoneal mice for the metastatic assay. After four weeks, mice were sacrificed, their tumor was isolated, the weight of xenografts was examined, and the numbers of metastatic nodules were counted. All animal studies were approved by the Institutional Animal Care and Use Committee of Chongqing Medical University, and carried out according to institutional guidelines for animal experimentation protocols (NIH publications Nos. 80-23, revised 1996).

In vivo tumorigenesis drug treatment

To assess the role of AKAP8 on ovarian cancer treatment with PARP inhibitor *in vivo*, xenografts models were established using female immunodeficient nude mice (Balb/c) that were 4 to 6 weeks old. OVCAR3 cells infected with different shRNAs were divided into shNC and shAKAP8 groups.The mice were injected with 5×10^6 cells subcutaneously on the back . After 6 days of tumor growth, the mice were divided into three groups: shNC + control, shAKAP8 + control, and shAKAP8 + niraparib. Niraparib was administered by gavage at a dose of 50 mg/kg. 0.5% of methyl cellulose was use as a control. Two weeks after, mice were sacrificed,the tumor diameters were measured with a slide caliper and the tumor's volumes were calculated as follows: volume = $(D\times d^2)/2$, where "D" meant the diameter with the longest length and "d" meant the diameter with the shortest length.

Cell transfection

For the generation of overexpression, OVCRA3, and SKOV3 cells were plated in a 6-well plate to reach 60-70% of confluence at the time of transfection. AKAP8 (wt or delete) or hnRNPUL1 long or short isoform (experimental group) and pENTER or pcDNA3.1 (control group) were added to the target cells (OVCRA3, SKOV3, and HEK293T), using jet PRIME transfection reagent (Polyplus, France) as described above and were incubated with 5% of CO_2 at 37°C 48 hours later, cells were collected for processed cell analysis.

Lentiviruses

HEK293T cells were transfected using the Polyplus transfection method to produce lentiviruses. Using the jet PRIME transfection reagent (Polyplus, France), lentiviral vectors were co-transfected into HEK293T cells together with the packaging vectors psPAX2 (#12260, Addgene) and pMD2.G (#12259, Addgene). Infectious lentivirus particles were collected after 48 hours and filtered using 0.45 μm PVDF filters.

Western blot

Using Cell Lysis buffer (Beyotime, China), the protein was extracted from the cells. Each group received the proper amount of cell lysate, which was added, thoroughly mixed with a vortex, and then put on ice for 30 minutes before being centrifuged for 10 minutes at 4°C at 12,000 rpm. Using a BCA protein quantification kit, the protein concentration was quantified. SDS-PAGE gel electrophoresis was used to separate the whole protein, and it was then transferred to a PVDF membrane. Primary antibodies were incubated on a horizontal shaker overnight at 4°C after the membranes had been blocked with 5% BSA in TBST for an hour. After washes, membranes were incubated with horseradish peroxidase (HRP)-conjugated secondary corresponding antibodies IgG mousse or rabbit. Immunodetection was performed with the enhanced chemiluminescence (ECL) detection Kit (Beyotime, China). The antibodies used in the present study were: anti-AKAP8 (Abcam, ab72196, 1:1000), anti-Flag M2 (Sigma, F3165, 1:2000), anti-hnRNPUL1 (Affinity, DF781, 1:1000), anti-PARP-1 (SCB, SB-8007, 1:500), anti-snRNP70 (Thermo Fisher, PA5-110406, 1:1000), anti-GAPDH (Proteintech, 10494-1-AP, 1:10000), anti-tubulin (Proteintech, 11224-1-AP, 1:1000), HRP-conjugated anti-mouse IgG, (Proteintech, SA00001-1, 1:10000), HRP-conjugated anti-rabbit IgG (Proteintech, SA00001-2, 1:10000).

Cell proliferation assay

To assess cell proliferation, the colony formation test and the Cell Counting Kit-8 assay (CCK-8) were used. Cells were seeded in a 96-well plate for the CCK-8 assay at a density of 4×10^3 per well, and incubated at 37°C for various lengths of time (0, 24, 48, 72, and 96 hours). By adding 10 μl of CCK-8 solution (DOJINDO, Japan) to each well of the plate, cell viability was determined. A microplate reader with a 450 nm setting was used to calculate the absorbance of each well. Three duplicates of each experiment were carried out. For colony formation

experiment,4×10^2 cells were seeded in each well six-well plates and the media was changed every three days. After 10 days and 12 days respectively for OVCAR3 cells and SKOV3 cells, colonies were fixed with 4% formaldehyde, stained for 30 minutes with 0.1% crystal violet (Sigma-Aldrich, USA), and then washed with PBS. Colonies' numbers were counted.

Transwell migration and invasion assays

A 24-well Transwell chamber system (Corning, USA) was used to conduct migration and invasion assay. For migration, in the upper chamber of the 24-well Transwell, 200 μl of suspension cells (4×10^4) in serum-free were seeded. In the lower chamber, 600 μl of culture media containing 20% FBS was added. For the invasion, 50 μl of Matrigel diluted with serum-free media was put into the upper chamber and incubated until solidification. Then 200 μl of suspension cells (4×10^4) in serum-free culture media were seeded in the upper chamber of the 24-well Transwell, and 600 μl culture media with 20% FBS were added to the lower chamber. Cells were fixed with 4% formaldehyde for 30 minutes after 24 hours of incubation and then stained for 2 hours with 0.1% crystal violet (Sigma-Aldrich, USA). The chamber membranes were mounted and covered on slides after being washed with PBS. Under a 200× microscope, migrated or invaded cells were visualized and counted.

RNA extraction and RT-PCR

Following the manufacturer's instructions, total RNA was extracted from cells using the TRizol reagent (Invitrogen, USA). The Prime Script RT Master Kit (Vazyme, China) was then used to generate cDNA from RNA. The Vazyme HI Script II One Step qRT-PCR SYBR Green Master Mix (Vazyme, #Q711, China) was used to amplify the reverse transcribed cDNA and assess the gene expression using the CFX96 real-time fluorescence quantitative PCR equipment system (Bio-rad, USA). Briefly, 1000 ng of RNA extracted were added to 4 μl of 4× gDNA into 14 μl of DEPC water, incubated for 2 minutes at 42°C then added 4 μl of 5× RT Super Mix and incubated at 50°C for 15 minutes and 85°C for 2 minutes. The qPCR reaction conditions was as follows: initial denaturation at 95°C for 2 minutes, followed by 40 cycles with 3 step PCR of 95°C for 10 seconds; 60°C for 30 seconds and 72°C for 30 seconds. Then the Melt cuve step (95°C for 15 seconds; 60°C for 1 minute and 95°C for 15 seconds). The relative expression of genes in each group of cells was calculated by the $2^{-\Delta\Delta Ct}$ method. The relative RNA expression level was normalized to GAPDH. The Table S2 displays the primer sequences that were used in this study.

Immunofluorescence and confocal microscopy

Cells were washed in PBS, fixed in 4% ice-cold paraformaldehyde for 15 minutes, and then washed again in PBS for immunofluorescence. Before being incubated with a 1:500 anti-AKAP8 antibody overnight at 4°C and developed with an HPR conjugated goat anti-rabbit secondary antibody for an hour at room temperature, cells were permeabilized with 0.1% Triton X-100/PBS for 10 minutes. The nuclear counter stain was performed using 4' 6-Diamidino-2-phenylindole (DAPI). An inverted fluorescence microscope was used to capture the fluorescence. Images were captured using a Zeiss LSM780 confocal microscope.

Nuclear and cytoplasmic separation

Briefly, after being trypsinized, fresh cells (5×10^6 cells) in a 10 cm dish were centrifuged at 800 g for 5 minutes at 4°C, washed with cold PBS, then separated into two tubes and processed for cell fractionation analysis. The cells were re-suspended in Buffer A (10 mM HEPES, 10 mM KCl, 1.5 mM MgCl2, 0.34 M sucrose, 10% glycerol), supplemented with 1 mM DTT (Sigma, USA), 5 mM sodium butyrate (Sigma, USA), and 0.1% Triton, and stood on ice for 5 minutes before being centrifuged at 1,300 g for 4 minutes at 4°C. A fresh tube was used to collect the supernatant (cytoplasm), which was then centrifuged at 12,000 g for 4 minutes at 4°C. After being dissolved in 1 ml of Buffer A and centrifuged at 1300 g for 4 minutes at 4°C, the pellet was added to 400 l of Buffer B (3 mM EDTA, 0.2 mM EGTA supplemented with 5 mM sodium butyrate and 0.1% Triton (Solarbio, China), maintained on ice for 30 minutes). The supernatant (nucleus) was centrifuged at 12,000 g for 4 minutes at 4°C following centrifugation at 1,700 g. To extract chromatin, the pellet was re-suspended in Buffer B after being washed with 1 ml of Buffer B, centrifuged at 10,000 g for 4 minutes at 4°C, and then sonicated. Finally, samples were collected from each group.

Immunoprecipitation (IP) and RNA immunoprecipitation (RIP)

IP and RIP assay was performed according to the manufacturer's instructions. Briefly, the medium was removed and cells were twice rinsed with PBS once they had reached 80% confluence. Cells were scraped, collected, and placed in 1.5 ml centrifuge tubes and centrifuged at 800 rpm for 5 minutes at 4°C. The pellet was resuspended in IP/RIP lysis buffer, which also contained RNase inhibitor/RNase A (CST, USA), DTT (Dithiothreitol), and a protease inhibitor cocktail (APExBIO, USA). After incubation on ice for 30 minutes, the lysate was collected by centrifugation at 12,000 g for 10 minutes at 4°C. The remaining lysate underwent immunoprecipitation with 2.5 g of anti-AKAP8 (Abcam ab72196), anti-Flag M2 (Sigma, F3165), anti-hnRNPUL1 (Affinity Ab-DF781), anti-CTCF (Abcam, ab128873), or corresponding control IgG (#NI01, Millipore) antibodies, followed by rotary agitation at 4°C overnight. The protein A/G Magnetic beads (Invitrogen, USA) was then added to the lysates and incubated for 4 hours at 4°C before being washed. Following the procedures outlined below, the protein was extracted, separated on an SDS-PAGE gel, and then examined by western blot. Immunoprecipitated RNAs were extracted using TRIzol (Invitrogen, USA) for RIP-qPCR analysis. In a nutshell, RNA was extracted using a TRizol reagent after being treated with DNase I for 5 minutes at 37°C The enrichment of RNAs was normalized to IgG.

RNA-seq and data analysis

Following the above-mentioned manufacturer's instructions, total RNA from OVCAR3 cells with AKAP8 down-regulated (shA8-1 and shA8-2), and two negative control groups were collected and extracted from each cell sample using the standard TRIzol method (Invitrogen, USA). Briefly, 2 μg of each RNA isolated from cells was dissolved in 10 μl of RNase-free and DNA digestion was carried out by DNaseI. RNA quality was determined by examining A260/A280 using Thermo's NanoDrop 2000. RNA Integrity was confirmed by 1.5% agarose gel electrophoresis. Using Sanger/Illumina 1.9 encoding, qualified RNAs were finally quantified and the quality control score was evaluated. The Agilent RNA Nano kit (Agilent Technologies,USA) was used to create RNA sequencing library following the manufacturer's recommendations using Agilent 2000 Bioanalyzer System. RNA Libraries were sequenced on the Illumina NovaSeq 6000 (Illumina) with PE150 model with paired-end 150 bp read length. Biodonductor package Deseq2 (applied biosystems/Thermo Fisher,USA) was use for RNA-seq analysis, followed DEXseq method to identify the differential exon usage in the cellular mRNAs.[30] TopHat (v2.0.13) was used to map each read to the human reference genome (GRCh38) and HTSeq (v0.6.0) was used to create read count tables. Two independent biological repeats were included in DEXseq. Only the exon usage changed two fold and the p value smaller than 0.05 between samples were defined as significantly used. All libraries were summarized in Supplementary Data and the RNA-seq data has been deposited in the NCBI database under the accession number: PRJNA843486.

Enhanced crosslinking immunoprecipitation followed by sequencing (eCLIP-seq)

eCLIP was carried out as previously described[29] with some minor modifications. Briefly, AKAP8-wt transfected in OVCAR3 cells was grown in RPMI 1640 media 10% FBS. When cells reached 80-90% of confluence, media was removed, and cells were washed twice with ice-cold 1× DEPC-PBS. Ice cold 1×DEPC-PBS was added, plates were placed on ice and irradiate once at 150 mJ·cm^{-2} at 254 nm for 30 seconds. Cells were scraped and harvested into Eppendorf tubes and centrifuged at 12 000 g for 20 seconds at 4°C. Cell pellets were resuspended in 1ml of CLIP lysis buffer [50 mm Tris-HCl, pH 7.4, 100 mm NaCl, 1% (v/v) Igepal CA-630, 0.1% (w/v) SDS, 0.5% (w/v) sodium deoxycholate] supplemented with 11 μl of protease inhibitor cocktail (200×), 5μl 0.1M DTT to 1 ml lysis buffer and sonicated once using a VibraCell probe sonicator for 20 s at 22% amplitude. Lysates were treated with 2 μl of Turbo DNase (Life Technologies, USA) for 3 minutes. At 37°C, shaking at 1,100 rpm, then immediately placed on ice. Samples were centrifuged for 10 minutes at 22 000 g at 4°C to clear the lysate. Each lysate were divided in two parts: IP1 and IP2 represent a part that the nucleic acid samples obtained by immunoprecipitation using the anti-FLAG antibody. Input1 and Input2 refers to the positive controls, which are lysate-derived nucleic acid samples. Protein G beads were previously washed twice in lysis buffer and then resuspended in 100 μl lysis buffer with the relevant antibody (3 μg anti-Flag; 3 μg anti-IgG) and incubated in rotation overnight with rotation at 4°C. The next day, 40 μl of protein G beads was added and incubated for 4 h, washed four times with a cold high-salt buffer [50 mmTris-HCl, pH 7.4, 1 m NaCl, 1 mm EDTA 1% (v/v) Igepal CA-630, 0.1% (w/v) SDS, 0.5% (w/v) sodium deoxycholate] and twice in PK buffer (100 mmTris-HCl pH 7.4; 50 mm NaCl; 10 mm EDTA). To digest the protein covalently bound to the RNAs and release peptide-RNA complexes, beads were resuspended in 50 μl PK buffer and 5 μl proteinase K, followed by incubation in shaking at 1100 rpm for 30 minutes at 37°C and transferred to nitrocellulose membranes using Nupage 4-12% Bis-Tris protein gels. RNAs on nitrocellulose were harvested, extracted then the First-strand cDNA synthesis was performed using a Superscript III Reverse Transcriptase kit (Thermo Fisher, USA) according to the manufacturer's instructions. Excess contaminating DNA was removed by on-column DNase digestion using the RNase-Free DNase Set (Thermo Fisher, USA). cDNA libraries were then prepared and sequenced using Illumina as described below. Antibodies used were as follows: anti-Flag M2 (Sigma, F3165), anti-mouse IgG (Proteintech, SA00001-1). eCLIP-seq data has been deposited in the NCBI database under the accession number: PRJNA1093080.

Chromatin immunoprecipitation (ChIP) assay

The manufacturer's instructions for the ChIP assay (Cell Signaling Technology, CST, USA) were followed. Cells were cultivated to 80-90% confluency in RPMI 1640 medium with 10% FBS. After 10 minutes of formaldehyde fixation, glycine was added to terminate the process. After that, cells were scraped off and harvested using centrifugation (2,000 g, 4°C, 5 minutes). The pellet was re-suspended in ChIP cell lysis buffer and incubated for 10 minutes on ice, being stirred by inverting every 3 minutes. The supernatant was then discarded. Micrococcal nuclease is used to fragment the pelleted nuclear material after centrifugation of the nuclei at 4°C, 2,000 rpm, for 5 minutes. The pellet was sonicated after being re-suspended in the ChIP buffer. Immunoprecipitations were performed by adding antibodies into digested chromatin overnight at 4°C. The samples were re-suspended in protein G magnetic beads and incubated for 2 hours. Beads were then washed with ChIP buffer. The DNA was purified using DNA purification spin columns. The enrichment of particular DNA was submitted to standard PCR. Antibodies used were as follows: anti-AKAP8 (Abcam, ab72196), anti-Poly II (Abcam, ab19346), anti-CTCF (Abcam, ab188408), and anti-H3K4me3 (Abcam, ab213224). The Supplementary Table displays the primer sequences that were used in this study.

Dual-luciferase reporter assay

In accordance with the manufacturer's recommendations, luciferase activity was detected using a dual-luciferase reporter assay kit (TransDetect, China). Briefly, cell lysis buffer was used to collect cells at 4°C, 12,000 rpm for 10 minutes. To measure fluorescence activity, 10 μl of supernatant in each 96-well opaque plate was mixed with 50 μl of Luciferase reaction reagent I in each well plate, incubated in darkness, then immediately recorded the firefly luciferase activity. Following the addition of 50μl of luciferase reaction reagent II to each well, the

plate was incubated in the dark, and the activity of Renilla luciferase was then measured by chemiluminescence. By dividing luciferase firefly activity over renilla activity, relative reading was obtained.

QUANTIFICATION AND STATISTICAL ANALYSIS

Graph-pad Prism was used to construct statistics and repeatability graphs. All quantitative data were expressed as the mean values standards deviation (SD) of at least three independent experiments. The Student's t-test was used to assess significant differences between the two groups, and analysis of variance (ANOVA) was used to compare differences between more than two groups. It was considered statistically significant when the P-value was less than 0.05. Significance was set at $P < 0.05$ (*), < 0.01 (**), or < 0.001 (***).